FINAL REPORT
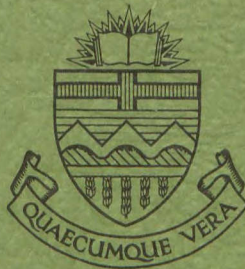
Research into Correlation of ISIS 2 Top-side Sounder and Energetic Particle Data with Ground-Based Magnetometer Data to Determine the Causes of Net Field-Aligned Current Flow in the Earth's Magnetosphere

DOC Contract No.   1SU 76-00020

DSS File Number   01SU.36100-5-0965

QUAECUMQUE VERA

Institute of Earth and Planetary Physics

DEPARTMENT OF PHYSICS

The University of Alberta
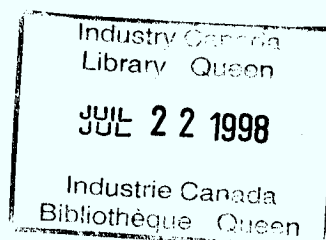
Edmonton, Alberta, Canada

NOV 14 1978

FINAL REPORT

Research into Correlation of ISIS 2 Top-
side Sounder and Energetic Particle Data
with Ground-Based Magnetometer Data to
Determine the Causes of Net Field-Aligned
Current Flow in the Earth's Magnetosphere

DOC Contract No.   1SU 76-00020
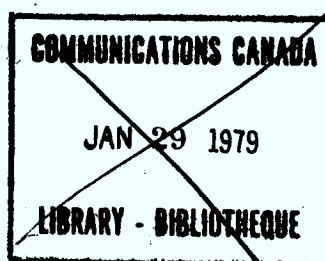
DSS File Number   01SU.36100-5-0965

Principal Investigator: _____
                        Dr. Gordon Rostoker

Co-Investigator: _____
                 Dr. Jerry L. Kisabeth

August 15, 1977

Abstract

The magnetic signatures of field-aligned and ionospheric currents can be used to determine the geometry and strength of the electrical current systems which couple the ionosphere to the outer regions of the earth's magnetosphere. It is now recognized that the currents flowing in the evening sector are an important clue to the understanding of processes leading to explosive substorm instabilities and episodes of intense ionospheric disruption. In this report we have used a combination of ground based magnetometer data and ISIS 2 satellite data in the form of energetic particles, auroral luminosity and electromagnetic and/or electrostatic noise measurements to provide a comprehensive picture of processes which are taking place on field lines penetrating the auroral oval in the evening and midnight sectors. We shall show that noise measurements in the frequency range $100 < f < 500$ kHz are characteristic of regions of upward current flow which are found in the region of discrete auroral features. We find no characteristic relationship on a one-to-one basis between the noise and thermal plasma enhancement at ISIS 2 altitudes. We find that the higher energy electrons (a few keV) are associated with the higher frequency noise. In addition, the highest noise frequencies are found in the center of discrete auroral arc regions with the frequency decreasing on either side of the center of the arc region. We believe that the source of noise in this frequency range is associated with electron beams in discrete auroral arcs whose velocity space distribution contains a region of positive slope. This distribution thus allows the electrostatic whistler noise to be convectively amplified.

Introduction

It is now well known that the interaction between the solar wind and its imbedded magnetic field with the earth's magnetic field results in a distortion of the magnetic field and the provision of energy for the ambient charged particle background. The magnetic field configuration, or magnetosphere, is shown in Figure 1 together with the various particle populations inside the magnetopause. The two regions of particular interest insofar as the solar-terrestrial interaction is concerned are the polar cleft, where magnetosheath plasma is thought to penetrate to the high latitude ionosphere, and the plasma sheet whose field lines thread the nightside auroral oval. At the present time it is felt that plasma from either the plasma mantle (Rosenbauer et al., 1975; Philipp and Morfill, 1976) or the entry layer (Haerendel and Paschmann, 1975; Paschmann et al., 1976) enters the magnetotail to eventually become part of the plasma sheet. However it is still necessary to seek mechanisms for accelerating electrons from the magnetosheath to energies which are adequate for the production of auroras in the E-region of the ionosphere.

One way of energizing auroral electrons which has recently generated great interest is the phenomenon of parallel electric fields. Several mechanisms have been proposed which may produce parallel $\underline{E}$ fields; they are:

(1) Double layers (Block, 1972, 1975) which are laminar non-turbulent potential drops whose thickness scales as the Debye length.

(2) Oblique electrostatic shocks (Swift, 1975) which are laminar non-turbulent potential drops whose thickness scales as the Larmor radius.
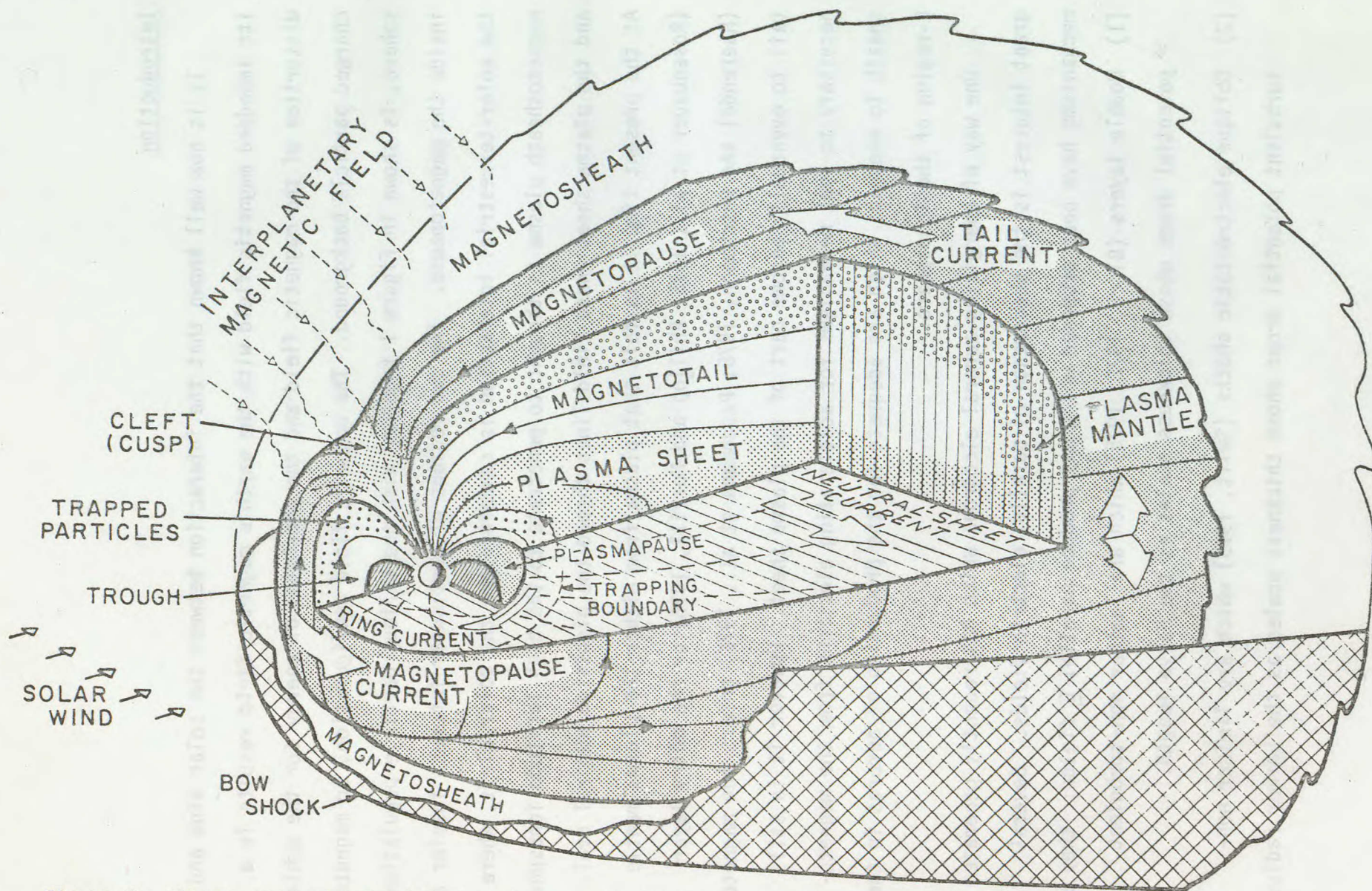
Figure 1: Three-dimensional diagram of the magnetosphere and the associated trapped particle populations (modified from an earlier version by Heikkila (1972)). The recently proposed entry layer lies just inside the magnetopause, and is not shown on this diagram.

(3) Anomalous resistivity (Hasegawa, 1974; Papadopoulos, 1977) which produces potential drops through the phenomenon of wave-particle interactions which produce turbulence in the plasma.

(4) Differences in pitch angle distribtuions between energetic ions and electrons (Alfvén and Fälthammar, 1963; Lennartsson, 1976).

(5) Induction electric fields in the magnetotail caused by rapid rate of change of the tail magnetic field associated with substorms (Heikkila and Pellinen, 1977).

Of these possibilities, (1), (2) and (3) have recently attracted great interest because of the discovery of strong parallel electric fields in the altitude range 3,000 - 10,000 km by the quite independent techniques of double-probes (Mozer et al., 1977) and barium cloud releases (Wescott et al., 1976). In addition there has been evidence, for some time, of significant parallel electric fields below the F-region peak (Mozer, 1976) particularly associated with auroral arcs. Finally we note that Evans (1974) has shown that the energy spectrum of electrons observed in the auroral zone ionosphere is what might be expected if there were a region of potential drop above the ionosphere.

In order to distinguish among the various possible mechanisms for the production of parallel $\underline{E}$ fields, it is useful to search for a possible diagnostic tool. One such tool is electromagnetic or electrostatic noise, which one might expect to be associated with plasma turbulence. For some time it has been known that noise in the range 100 - above 500 kHz is observed at altitudes of $\sim$ 1400 km in the vicinity of the auroral oval (Hartz, 1971). Association of the noise with the energetic particle distribution and electric

current configuration might allow us to comment on the character and loca-
tion of any regions of electric potential drop which might involve plasma
turbulence responsible for the generation of the noise. One of the primary
purposes of this research is to pursue the aforementioned approach. We
shall show that correlation of the energetic particle fluxes and noise along
with the thermal plasma density measured by ISIS 2 can be correlated with
electrojet current distributions over which ISIS 2 passes to yield important
information on the nature of the acceleration of auroral particles.

Data Utilized in this Study

Any effort to understand the mechanisms for the generation of magneto-
spheric and ionospheric phenomena must, of nature, involve several suites
of complementary data. In this study we shall refer to the following data:

(i) Ground-based magnetic data

Values of the three magnetic field components (H, D, Z) were available
from the University of Alberta meridian line (see Table 1) over the interval
November 1971 - March 1972. The data sample rate was once per component
every two seconds, and values were accurate to ±1 nT. Timing was achieved
using a WWVB time code receiver and was accurate to ±0.1 sec. The data at
a given instant of time during each ISIS 2 pass were sampled, and latitude
profiles were constructed. A simple coordinate transformation allowed the
data to be plotted as a function of geomagnetic latitude (which is almost
identical to invariant latitude along the Alberta meridian line). The latitude
profiles were interpreted to infer the positions of poleward and equatorward
borders of the eastward and westward electrojets which flowed in the longi-
tudinal sector traversed by the ISIS 2 satellite.

Table 1

Coordinates and L Values of Magnetometer Line Sites

Site	Geographic		Geomagnetic		L R_E
	Latitude (°N)	Longitude (°E)	Latitude (°N)	Longitude (°E)	
Resolute Bay	74.7	265.1	83.0	289.4	71.4
Cambridge Bay	69.1	255.0	76.8	296.6	19.5
Contwoyto Lake	65.5	249.7	72.6	295.8	11.3
Fort Reliance	62.7	251.0	70.3	300.1	8.9
Fort Smith	60.0	248.0	67.3	300.0	6.8
Fort Chipewyan	58.8	248.0	66.3	303.1	6.2
Fort McMurray	56.7	248.8	64.2	303.5	5.4
Meanook	54.6	246.7	61.9	300.8	4.5
Leduc	53.3	246.5	60.6	302.9	4.2

(ii) Electromagnetic or Electrostatic Noise

Noise in the frequency range 100 - 500 kHz was measured aboard the ISIS 2 spacecraft using the automatic gain control (AGC). The range of this device is from 0 to -105 db as it sweeps across the relevant portion of the frequency band in the space of $\sim$ 1 sec. Care was taken in the interpretation of these data due to the frequent appearance of a contribution to the "noise level" associated with the Z-wave cutoff and the local plasma frequency. The time between noise samples varied, depending on whether or not the satellite was functioning at a high sample rate or not as regards the topside sounder; at best the satellite travelled $\sim$ 0.6° of latitude between samples and at worst $\sim$ 1.2° of latitude for the data utilized in this study (see Table 2 for list of ISIS 2 passes used).

(iii) Energetic Particle Precipitation

Particle fluxes in the energy range 5eV < E < 12 keV were available from the soft particle spectrometer (SPS) aboard ISIS 2, courtesy Dr. J. D. Winningham. The data are presented in the form of spectrograms (including values of number flux and energy flux) and differential energy spectra in which dJ/dE is plotted as a function of particle energy E (J being the particle flux). The data are effectively continuous, although different pitch angles from 0 - 180° are sampled sequentially.

(iv) Auroral Luminosity

This information was abstracted from a paper by Wallis et al. (1976) in which ISIS 2 scanning photometer data were portrayed to show the correlation between the auroral electrojets and auroral luminosity. The photometer data were used to define the position and latitudinal extent of several

Table 2

Times, K_p and Geographic Longitudies of ISIS 2 Passes Used in this Study

Year	Day	UT (when satellite was at ~ 70° Latitude)	Geographic Longitude of Pass (°W) nearest Alberta Chain of Stations	Level of Magnetic Activity (K_p)
1971	346	0609	103	1-
	349	0608	109	1-
	360	0529	110	4-
1972	003	0450	108	1o
	004	0527	120	3o
	005	0412	102	2o
	010	0334	101	1o
	011	0410	108	4-
	013	0333	103	1-
	017	0409	115	4o
	018	0254	97	4o
	019	0332	109	3-
	025	0331	115	4-
	030	0252	110	3+
	032	1512	111	2+
	038	0213	109	2o
	039	0250	120	3-
	040	1432	110	0+
	041	0213	112	3o
	048	1354	110	4+
	052	0133	116	2+
	053	1314	106	1o
	054	0055	108	1+
	058	1236	102	1o

intense auroral forms at times corresponding to some of the ISIS passes used in this study. It should be noted that the arcs defined in this section are often rather broad (up to 2° in latitudinal extent) and thus the positions shown in this study represent the average locations only.

(v) Thermal Plasma Density at 1400 km

Thermal plasma densities at satellite altitude can be estimated by evaluating the local plasma frequency f_N which is related to ambient plasma densities through the relationship

$$n_e = \left(\frac{f_N}{8.98 \times 10^3} \right)^2$$

where f_N is in Hz and n_e is in particles per cubic centimeter.

In an earlier study, Rostoker et al. (1975a, 1976) have estimated the positions of thermal plasma enhancements at 1400 km for many of the passes treated in the present study. Such information is useful in that cold plasma may regulate the operation of plasma instabilities which can result in the generation of electromagnetic and electrostatic noise.

Events Treated in this Study

Three types of situations are dealt with in the following study:

(1) The satellite traverses a purely eastward electrojet in the evening sector; if there is a weak westward electrojet to the north, it cannot be identified from the ground-based data.

(2) The satellite traverses both the eastward electrojet and an identifiable westward electrojet to the north in the evening sector.

(3) The satellite traverses a purely westward electrojet in the morning sector.

Figure 2 shows a polar plot of the electrojets and pass types mentioned above. A bar plot showing the latitudinal distribution of the electrojets for each event, along with the noise distribution for frequencies in the range $100 < f < 500$ kHz with intensities above -70 db and the boundaries of thermal plasma enhancements at satellite altitude is shown in Figure 3. In the following sections we shall discuss several typical events from the sample size described in Figure 3. We shall concentrate on eastward electrojets in the evening sector, as they constitute the major portion of the events treated in this study.

Case 1   Eastward Electrojet in the Late Evening Sector
         Day 346, 1972   Start Time 0605 UT

We shall treat this event in considerable detail, as a large amount of additional correlative data were available in this case. In following cases we shall emphasize points of agreement with this first case, and try to point out any inconsistencies should they arise.

The ISIS 2 spacecraft was on a southbound pass along geographic meridian $\sim 104°W$ ($\sim 7°$ east of the Alberta meridian line). The topside sounder was in the fast sweep mode, yielding an ~ 14 sec. resolution for noise data across the auroral oval. In Figure 4 we show the latitude profile of the ground magnetometer data. It reveals an eastward electrojet of ~ 680 km in latitudinal extent in the latitude range $65° < \Lambda < 71°N$ with a peak magnetic perturbation of < 45 nT. This profile was stable over the interval of the pass. The shaded bar on the profile represents the location of noise whose
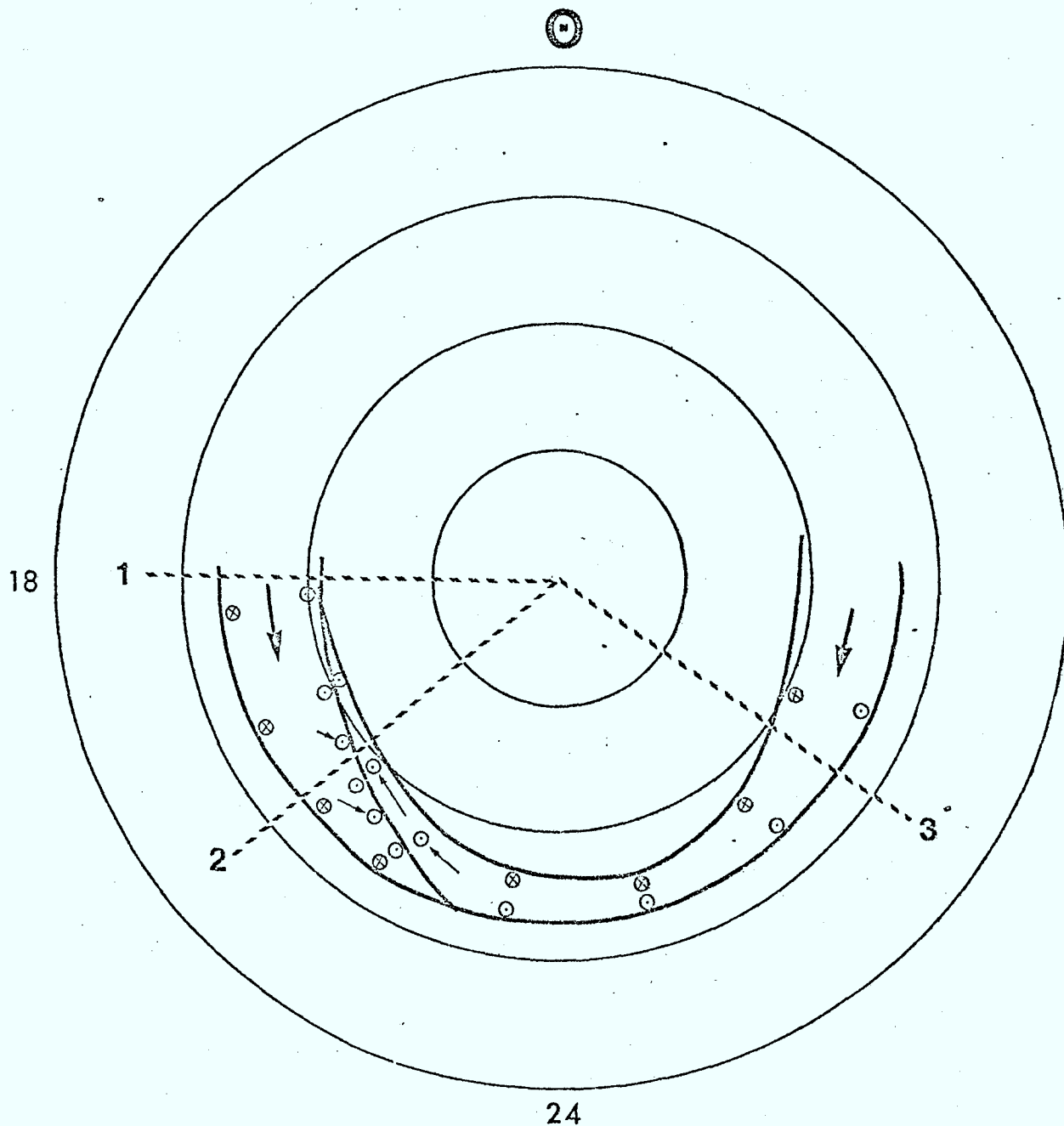
Figure 2: Polar plot of the ionospheric and field-aligned currents in the
nighttime sector. Upward field-aligned currents are shown by ⊙ and down-
ward currents by ⊗ . The westward electrojet in the morning sector flows
across midnight and gradually diverges up the field lines into the evening
sector poleward of the eastward electrojet. Some current from the eastward
electrojet encounters the poleward boundary of the electrojet and diverges to
flow upwards along the field lines. Note the excess of upward compared to
downward current flow in the evening sector; this is the phenomenon of net
field-aligned current.
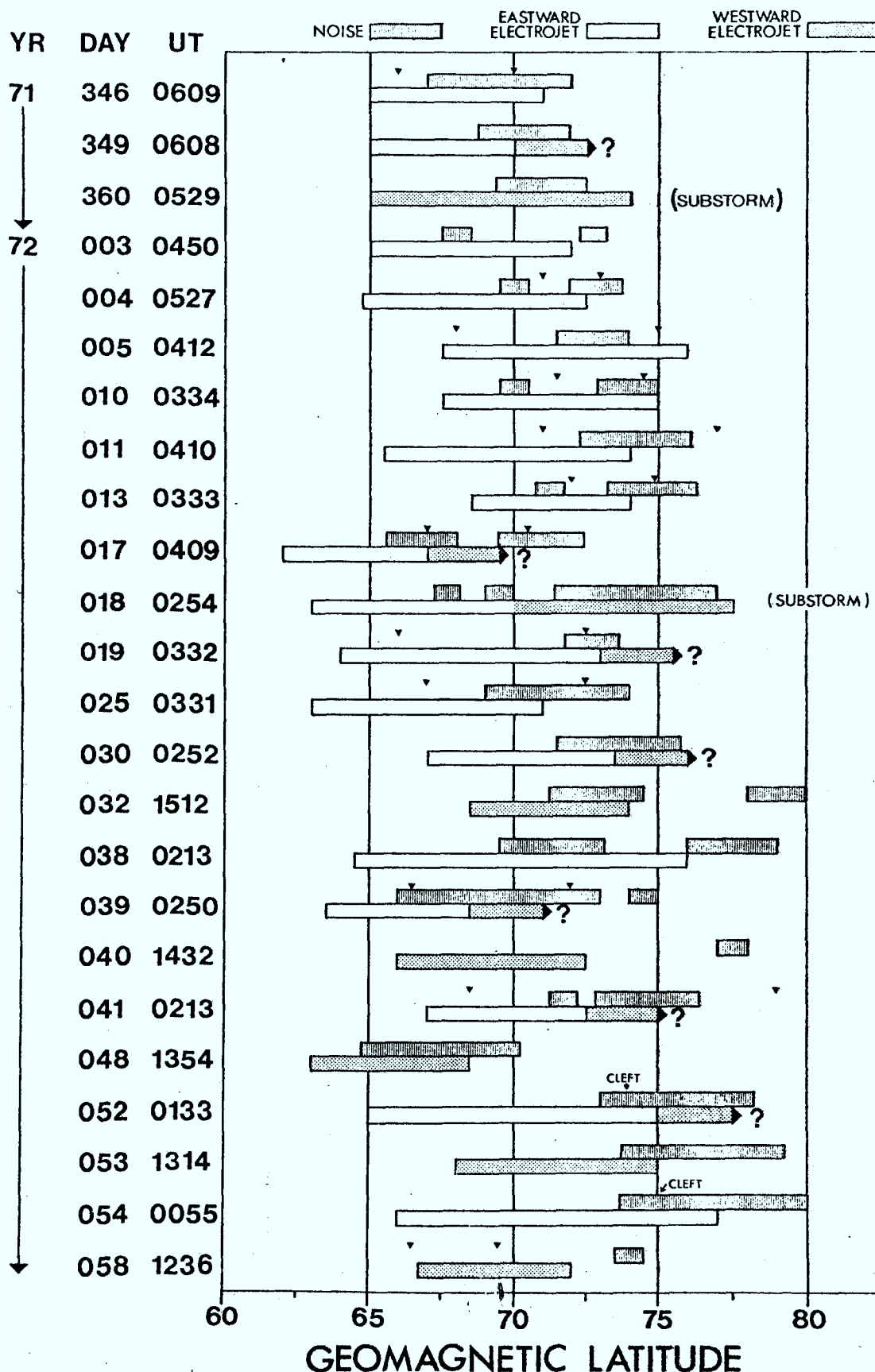
Figure 3: Summary plot of the latitudinal extent of eastward (open bars) and westward (dotted bars) electrojets. Also shown is the latitudinal extent of regions where noise amplitudes exceed -70 db (vertically hatched bars) and the boundaries of thermal plasma peaks for some events (indicated by small vertical arrowheads). For some westward electrojets poleward of the eastward jet, poleward borders were not easily identifiable. This is indicated on the plot by the symbol "?". For passes through the dayside cleft, the latitude of the associated thermal plasma enhancement is indicated by the term CLEFT.
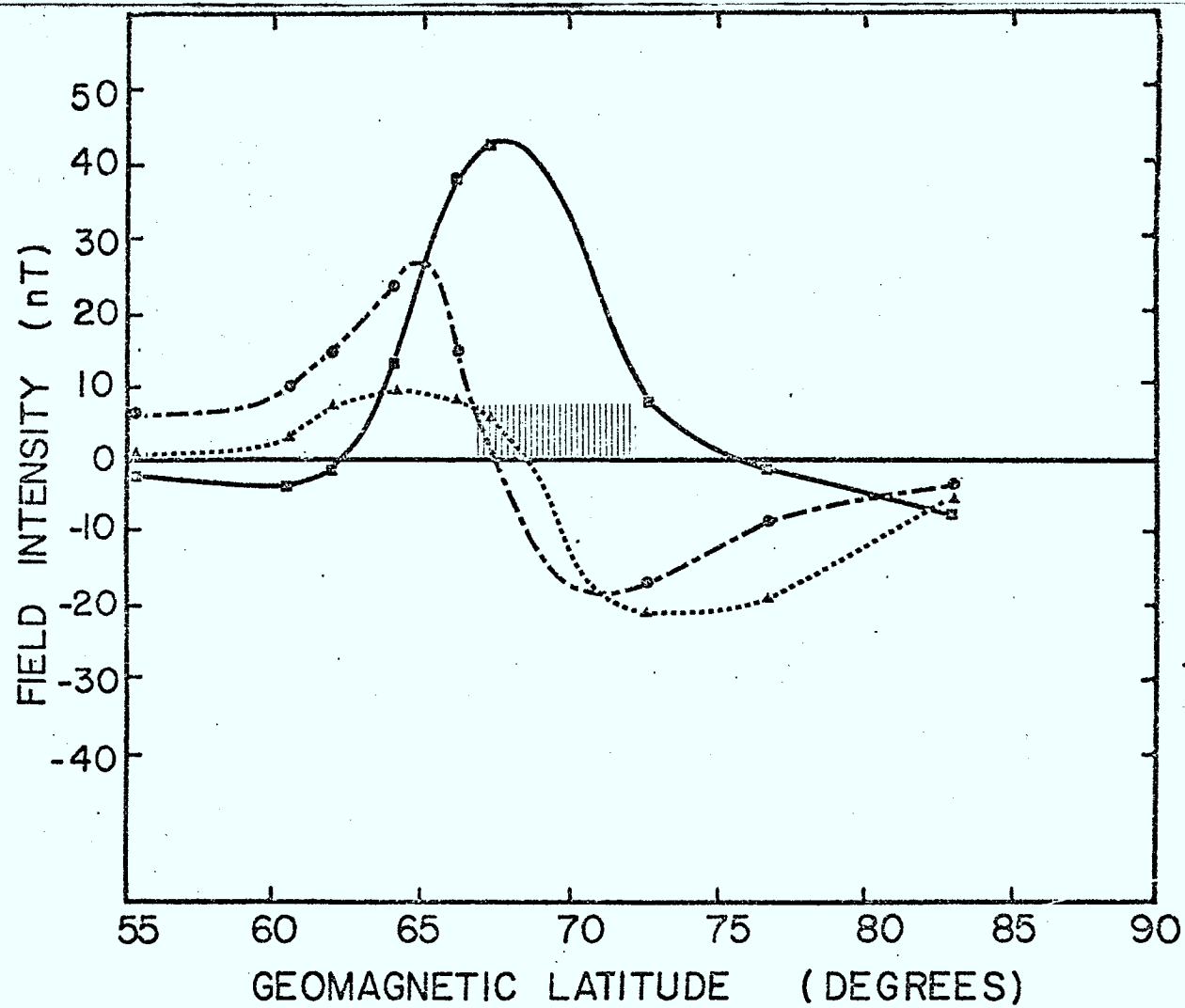
Figure 4: Latitude profile of the magnetic perturbation pattern along
the Alberta meridian line (see Table 1), for the event of
Day 346, 1971 at 0611 UT. The geomagnetic north component
is indicated by small squares, the geomagnetic east component
is indicated by small triangles and the vertical component
(positive downwards) is indicated by small solid circles.
The region of noise with amplitude greater than -70 db is
indicated by the vertically hatched bar.

amplitude exceeded - 70 db. The noise spectra are shown in Figure 5, on which the latitudinal extent of the eastward electrojet is indicated by the horizontal bar beneath the spectra. The amplitude scale of the noise is indicated in the lower panel as is the frequency scale which covers the range 100 < f < 500 kHz.

For this event, all-sky camera data from the high latitude station of Fort Smith (67.3°N) were available. These data revealed a diffuse aurora covering most of the sky over that station with a discrete arc lying approximately 260 km north of Fort Smith at ∿ 69.5°N. This arc appears to lie close to the poleward border of the eastward electrojet, and given the resolution of the magnetometer array at high latitudes, may well have been located at the poleward border of the eastward electrojet. There may have been arcs further poleward of 69.5°N, but the all-sky camera did not cover that field of view.

It can be seen from Figure 5 that the noise level built up steadily for approximately 200 km as the satellite approached the poleward border of the eastward electrojet. Up to that border the noise was confined to the frequency band 100 < f < 200 kHz. As the satellite crossed the poleward border of the eastward electrojet and approached the discrete arc, there was a marked increase in high frequency noise with the maximum bandwidth being attained approximately at the latitude of the discrete arc. Further passage southward resulted in a loss of the high frequency components with rather low noise levels being present in the equatorward portion of the electrojet. There seems to be a slight secondary peak equatorward of the main region of noise (spectrum 14); as we shall see in later examples, this secondary peak is a rather common feature for evening sector passes.
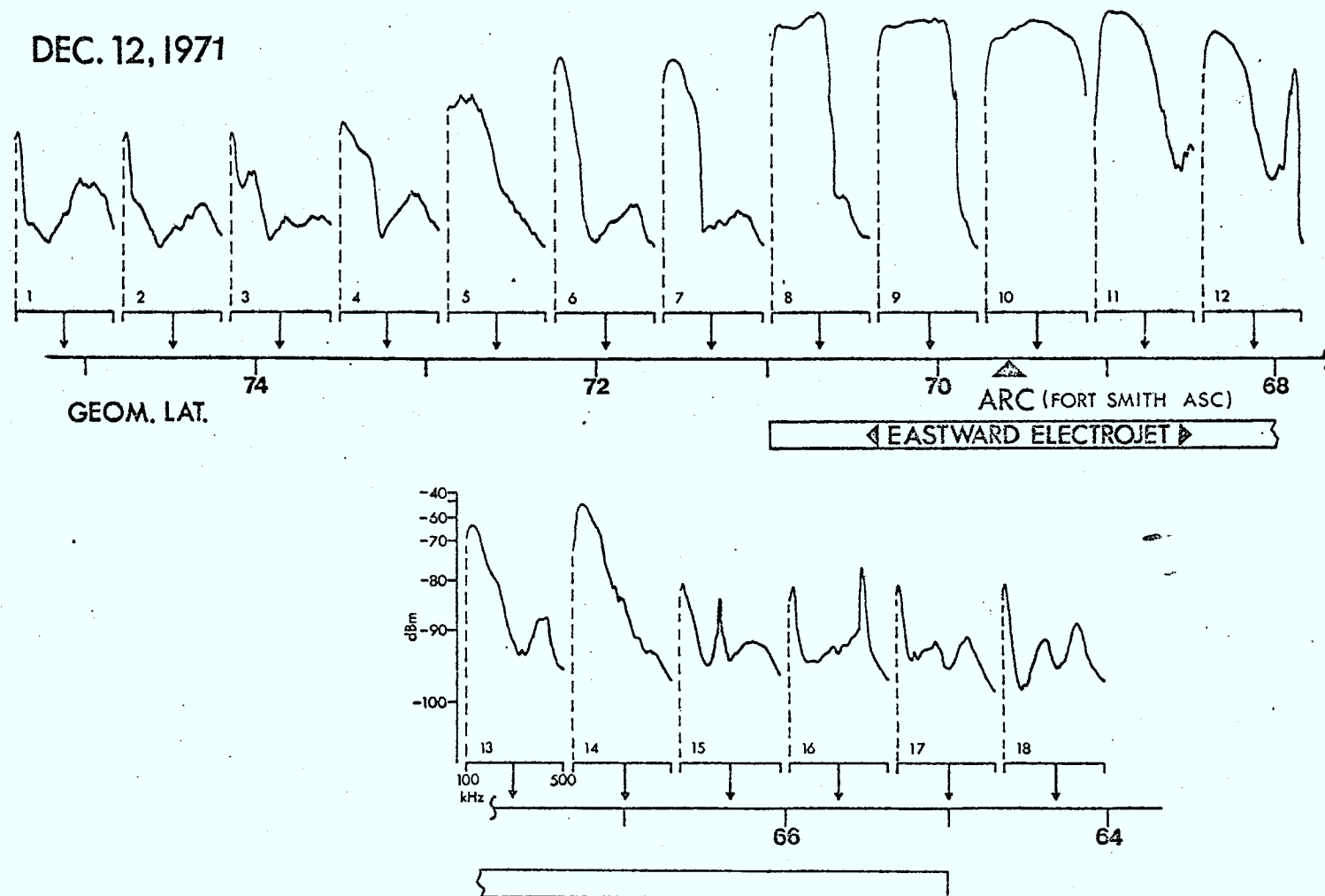
Figure 5: Spectra of noise measured by the AGC aboard the ISIS 2 spacecraft. The frequency range of 100-500 kHz is indicated on the abscissa of spectrum 13, while the amplitude range (-105 db to -40 db) is indicated on the ordinate of spectrum 13. Arc positions are indicated by arrowheads and appropriate labels. The electrojet is indicated by the horizontal bar below the spectra. These spectra are for Day 346, 1971 (December 12, 1971) for which Figure 4 shows the latitude profile.

In Figure 6 we show the spectrogram of energetic electrons measured by the soft particle spectrometer (SPS) aboard ISIS 2. The top panel shows the spectrum for electrons in the energy range 10 < E < 10,000 eV. The second panel shows the pitch angles of the particles being sampled (θ = 180° for the detector looking down the field lines sampling upcoming particles). The third panel shows the number flux while the fourth panel shows the energy flux. All quantities are plotted on a logarithmic scale. The abscissa shows the magnetic local time (MLT), invarient latitude and Universal Time of the pass. The times of individual noise spectra shown in Figure 5 are indicated on the Figure. The region of noise with amplitude greater than - 70 db is bracketed by spectra 8 - 14 inclusive. The appearance of the high frequencies (f > 200 kHz) clearly corresponds to the appearance of intense fluxes of electrons in the range of hundreds of eV to several keV over the latitude range 70° < Λ < 72°N. This region undoubtedly corresponds to the discrete arc detected by the all-sky camera ∿ 7° to the west of the satellite subtrack. The electron fluxes decrease markedly near 70°N and suffer a secondary enhancement (in the region of the previously mentioned secondary enhancement in noise level) around 66 - 68°N.
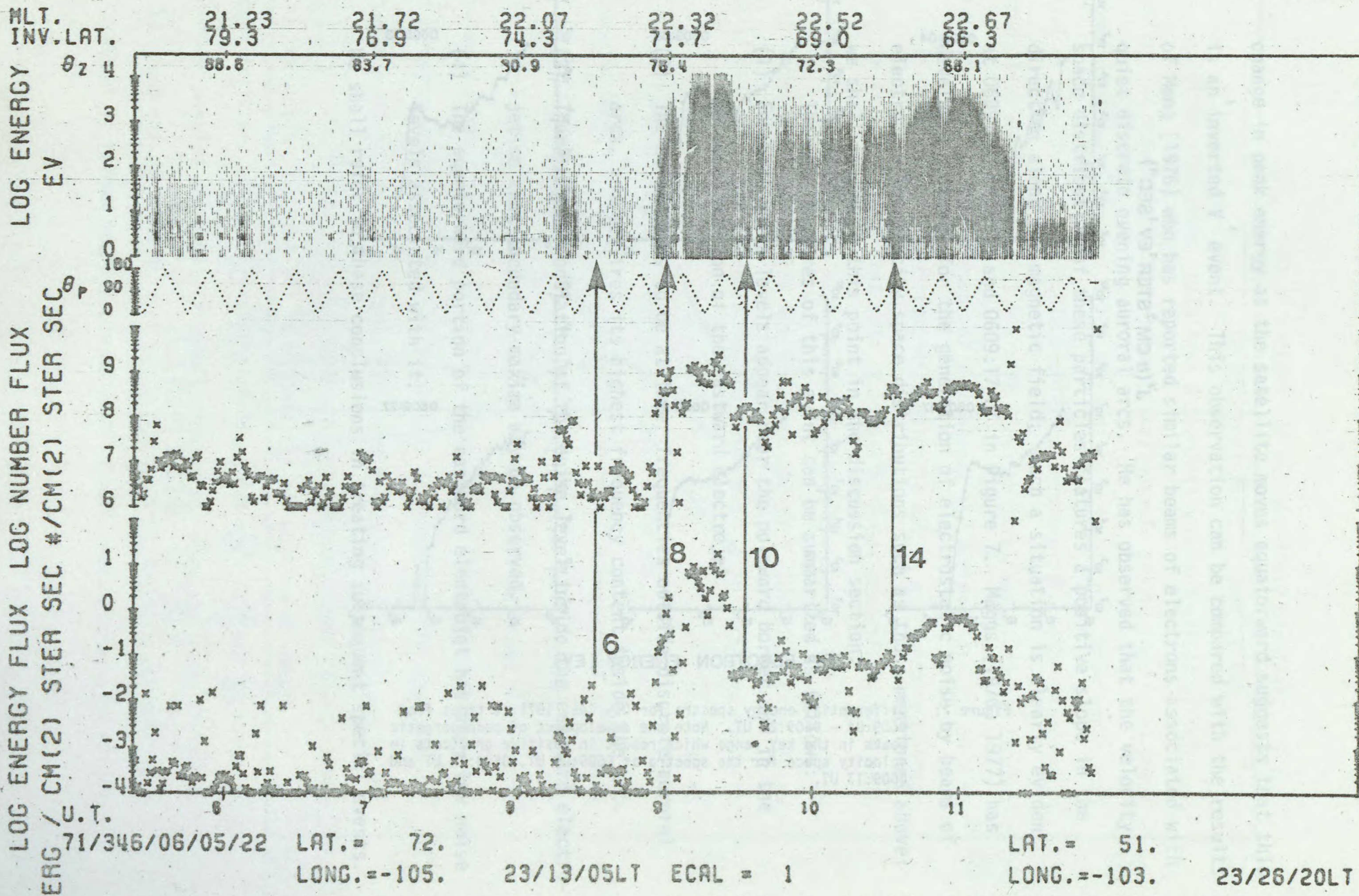
Based on these data, we would contend that the region between 70 - 72°N marks field lines on which energetic electrons are accelerated and noise is produced. We shall therefore look more closely at this region by presenting a series of differential spectra in Figure 7 covering the interval 0609:04 UT to 0609:27 UT which marks the passage of the satellite across the poleward boundary of intense electron precipitation, (see spectrum 8 in Figure 5). There is clearly a region where there is a relatively more energetic stream of electrons with peak energy fluctuating between 1-4 keV; the

Figure 6: Electron spectrogram for the soft particle spectrometer (SPS) aboard the ISIS 2 spacecraft. Energies are given on a grey scale with intense fluxes being shown by dark regions. The energy scale is logarithmic ranging from 10-10,000 eV on the top panel. The second panel shows the pitch angle distribution (for θ_p = 180° the detector points down the field lines and detects upward moving fluxes). The two bottom panels show number flux and energy flux respectively on a logarithmic scale. The vertical arrows refer to noise spectra shown in Figure 5. This spectrogram is for Day 346, 1971 for which Figure 4 shows the latitude profile.

TOP ELECTRON DATA   ISIS-II

MLT.   21.23   21.72   22.07   22.32   22.52   22.67
INV.LAT.   79.3   76.9   74.3   71.7   69.0   66.3
θz   88.6   83.7   80.9   78.4   72.3   66.1

LOG ENERGY / EV

θP

LOG ENERGY FLUX LOG NUMBER FLUX
ERG / CM(2) STER SEC #/CM(2) STER SEC

U.T.

71/346/06/05/22   LAT.=   72.   LAT.=   51.
            LONG.=-105.   23/13/05LT   ECAL = 1   LONG.=-103.   23/26/20LT

qMAX= 0.8   ORBIT= 3241 ALT.= 1433 N >= 0. TAPE NO. 1346AD DATE PROCESSED: 12-MAY-75
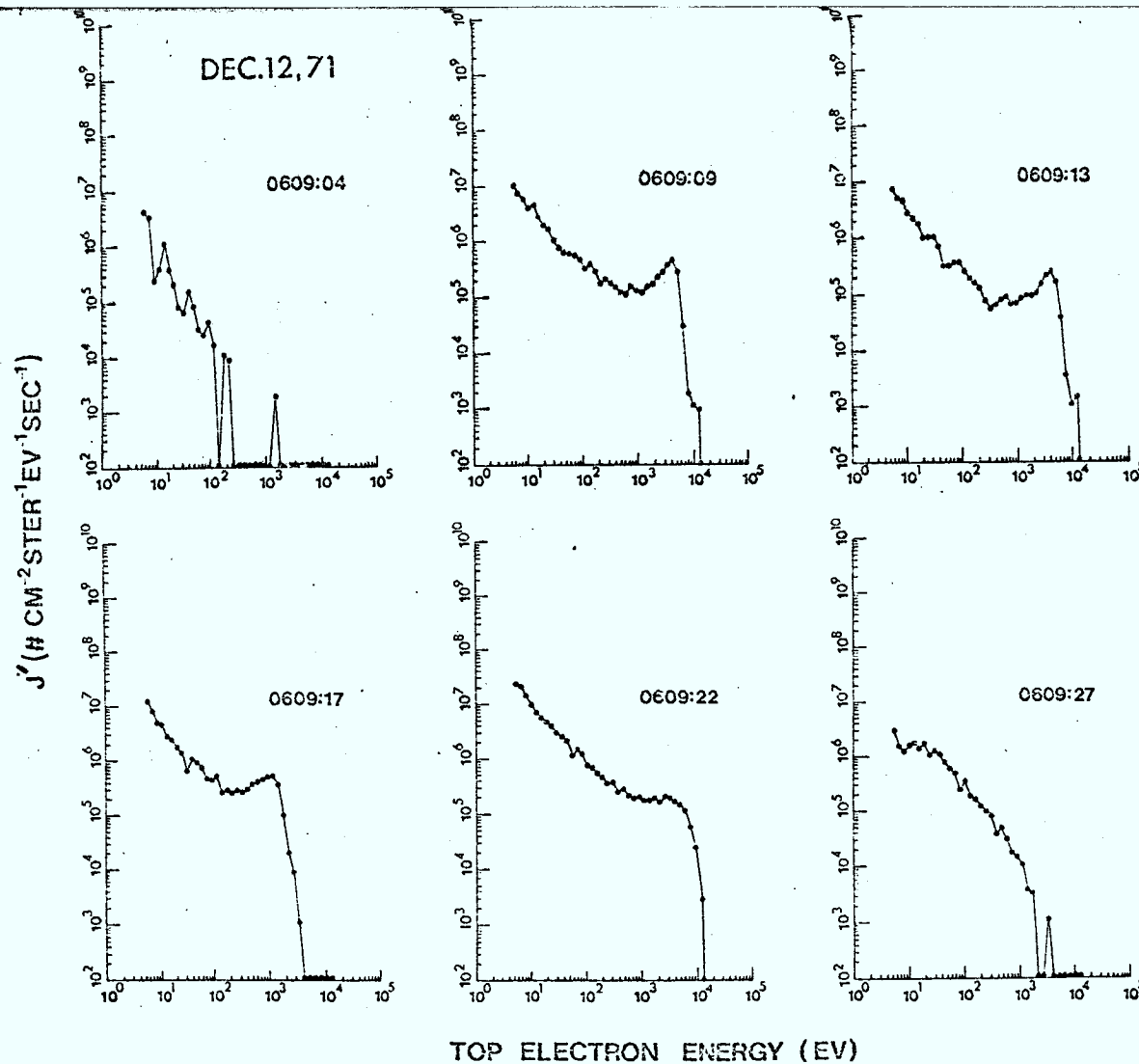
Figure 7: Differential energy spectra for Day 346, 1971 at times from 0609:04 - 0609:27 UT. Note the development of monoenergetic peaks in the keV range which result in positive gradients in velocity space for the spectra at 0609:09 UT, 0609:13 UT and 0609:17 UT.

change in peak energy as the satellite moves equatorward suggests that this is an 'inverted V' event. This observation can be compared with the results of Meng (1976) who has reported similar beams of electrons associated with quiet discrete evening auroral arcs. He has observed that the velocity space distribution of these particles features a positive slope in the direction along the magnetic field; such a situation is clearly evident at 0609:09, 0609:13 and 0609:17 UT in Figure 7. Maggs (1976, 1977) has developed a theory for the generation of electrostatic noise by beams of electrons with velocity space distributions such as those mentioned above; we shall return to this point in the discussion section.

The main features of this event can be summarized as follows:

(1) Enhanced noise levels appear near the poleward border and in the poleward portion of the eastward electrojet.

(2) The noise tends to be at lower frequencies outside discrete auroral arcs, and acquires its highest frequency content inside the arc.

(3) There may be modulation of the noise level inside the eastward electrojet so that secondary maxima may be observed.

(4) The equatorward portion of the eastward electrojet has very low noise levels associated with it.

We shall refer to these conclusions in treating subsequent special events.

Case 2   Eastward Electrojet in the Evening Sector

Day 4, 1972   Start time 0524 UT

The satellite was on a southbound pass along geographic meridian $\sim$ 120°W ($\sim$ 9° west of the station line), and the topside sounder was in the fast sweep mode. In Figure 8 we show the latitude profile of the ground magnetometer data. It depicts an eastward electrojet of $\sim$ 890 km in latitudinal extent in the latitude range 64 < Λ < 72°N with a peak perturbation of $\sim$ 60 nT. The profile was stable over the period of the pass. Again the shaded bar shows the region of noise with amplitude greater than -70 db. The noise spectra are shown in Figure 9. For this event, auroral arc positions as well as the latitudinal regime of the diffuse auroras were available from Wallis et al., (1976). The boundaries of the diffuse aurora originally obtained by Wallis et al. are corrected for albedo by shifting them by $\sim$ 1° of latitude.

As for case 1, the noise builds up in amplitude as the satellite approaches the poleward border of the eastward electrojet. A major noise intensification occurs between 73.5 - 74.2°N (spectrum 7) with the high frequencies becoming very strong; the high frequencies disappear briefly and then reappear near 72°N (spectrum 10). There is a clear secondary noise maximum near 70°N, although it is lacking in high frequencies compared to the higher frequency noise regimes. The equatorward half of the eastward electrojet is completely devoid of noise.

In Figure 10 we show the spectrogram of the energetic electrons measured by the SPS. The region of noise near 74°N would, on first sight, appear to correlate with the intense fluxes of electrons between 74-75°N (spectrum 7), although there is a curious lack of noise in the heart of the region of precipitation. There is, however, a clear region of intense
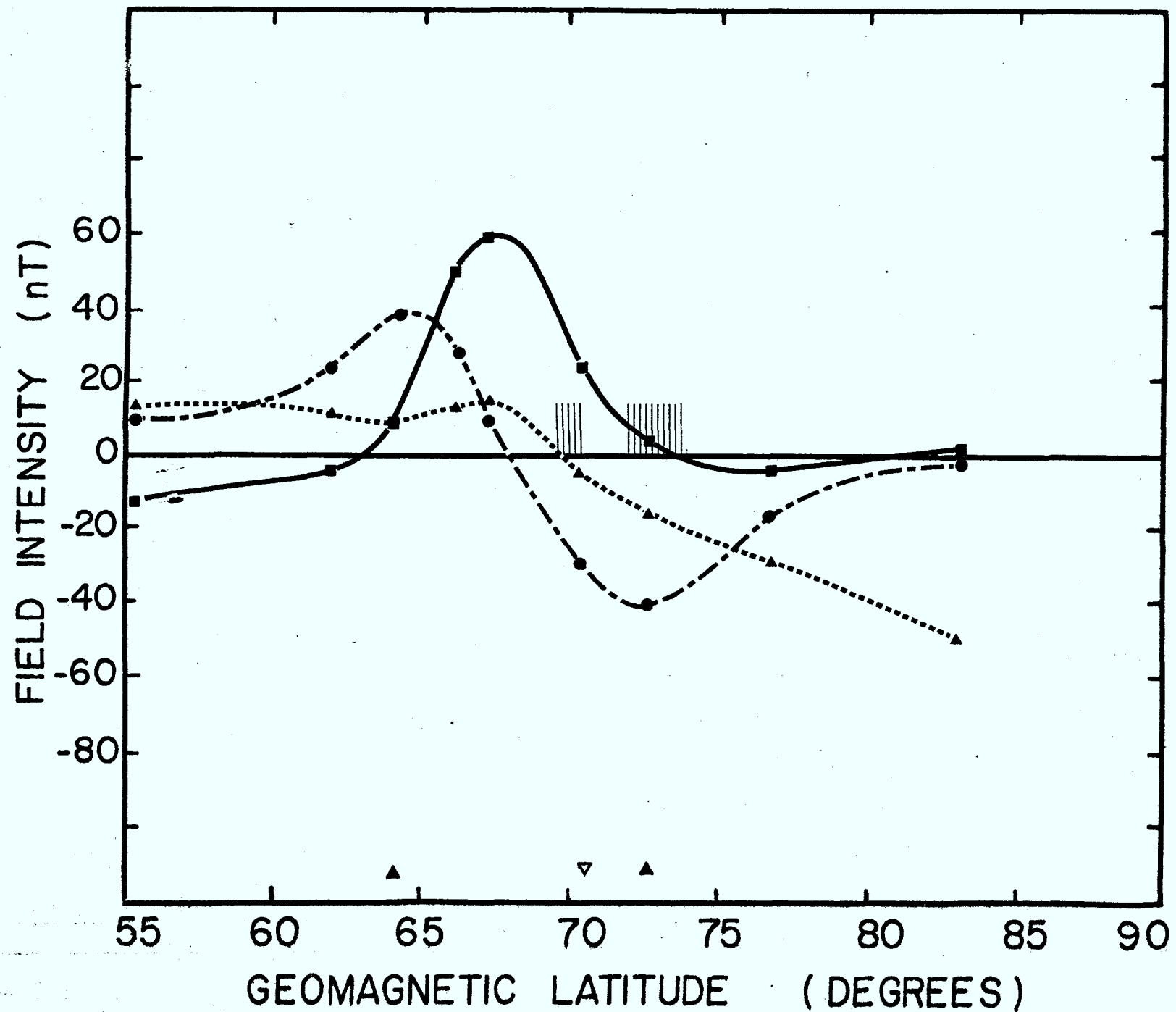
Figure 8:   Same as Figure 4 except for Day 4, 1972 at 0528 UT.

JAN. 4, 1972

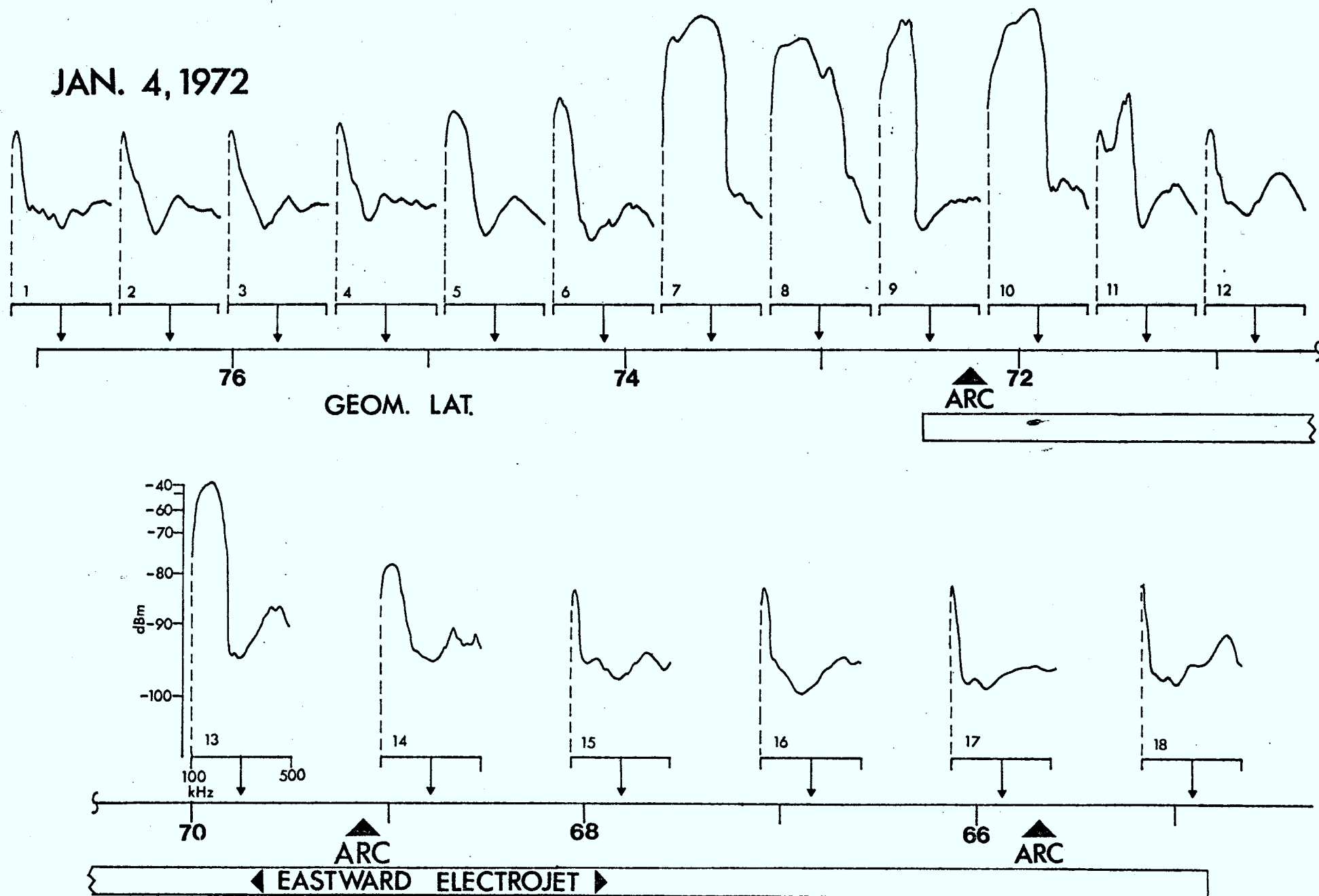GEOM. LAT.

ARC

dBm

100 kHz   500

EASTWARD ELECTROJET

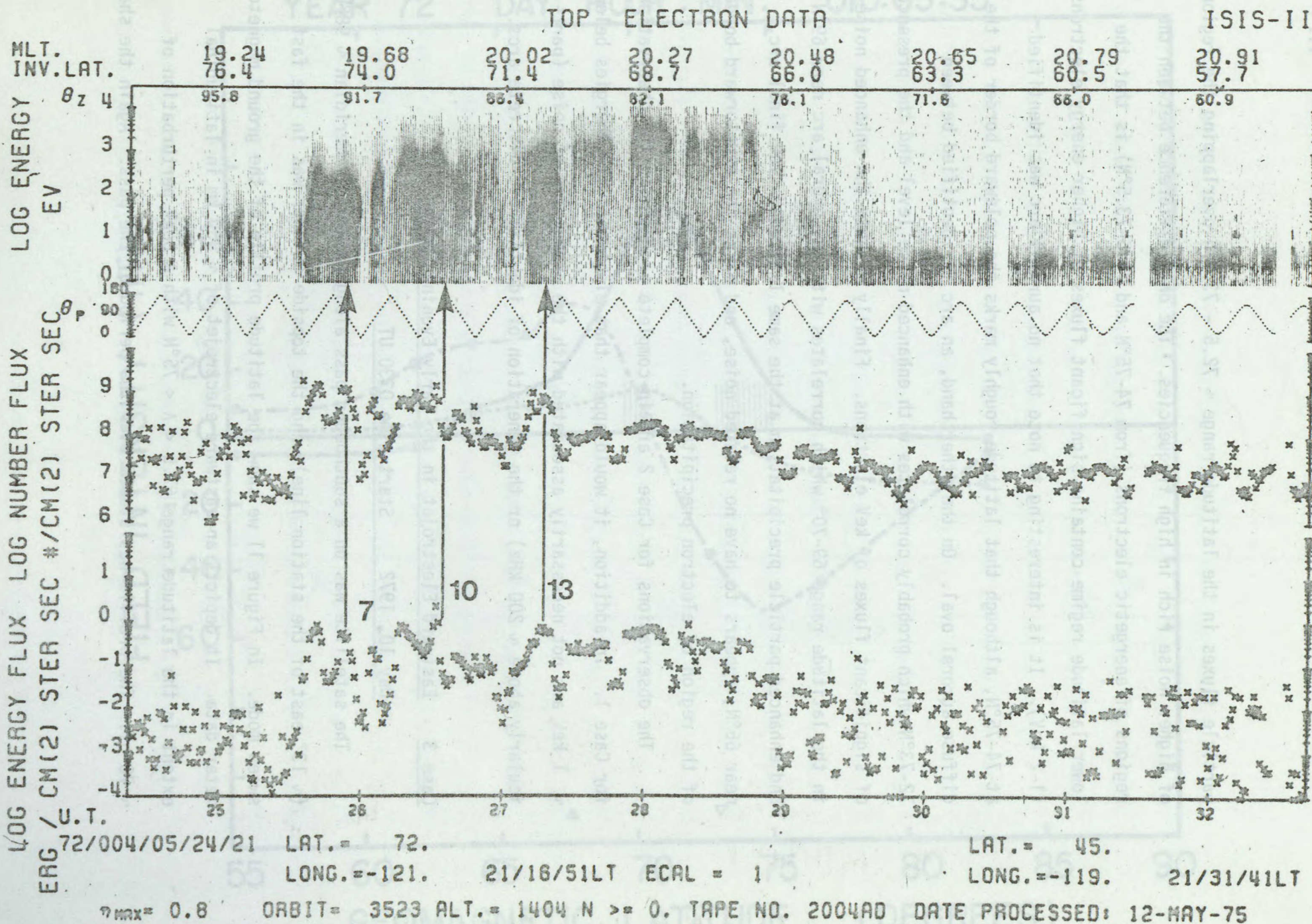Figure 9:   Same as Figure 5 except for Day 4, 1972 with start time
0524:21 UT.

Figure 10: Same as Figure 6 except for Day 4, 1972 with start time 0542:21 UT

particle fluxes in the latitude range ∿ 72.5 - 73.5°N overlapping the region of higher noise rich in high frequencies. The only difference between the regions of energetic electrons (from 74-75°N and 72.5-73.5°N) is that the lower latitude regime contains significant fluxes of higher energy electrons (1-2 keV). It is interesting to note that no auroral arc was identified at 74-75°N, although that latitude roughly marks the poleward border of the diffuse auroral oval. On the other hand, an arc is identified between 72-73°N which probably correlates with enhanced noise level and the presence of significant fluxes of keV electrons. Finally we note the enhanced noise in the latitude range 69-70° which correlates with an auroral arc near 69°N and enhanced particle precipitation at the same latitude. The final arc, near 66°N, appears to have no related noise, and marks the equatorward border of the region of electron precipitation.

The observations for Case 2 are in complete accord with the observations for Case 1. In addition, it would appear that electrons with energies below ∿ 1 keV are not necessarily associated with the production of noise (particularly above ∿ 200 kHz) or the generation of identifiable discrete arcs.

Case 3   Eastward Electrojet in the Early Evening Sector
          Day 10, 1972   Start time 0330 UT

The satellite was on a southbound pass along geographic meridian ∿ 98°W (∿ 13° east of the station line), and the topside sounder was in the fast sweep mode. In Figure 11 we show the latitude profile of the ground magneto-meter data. It depicts an eastward electrojet of ∿ 830 km in latitudinal extent in the latitude range $67.5 < \Lambda < 75°N$ with a peak perturbation of ∿ 70 nT. The profile was stable over the period of the pass. Again the shaded
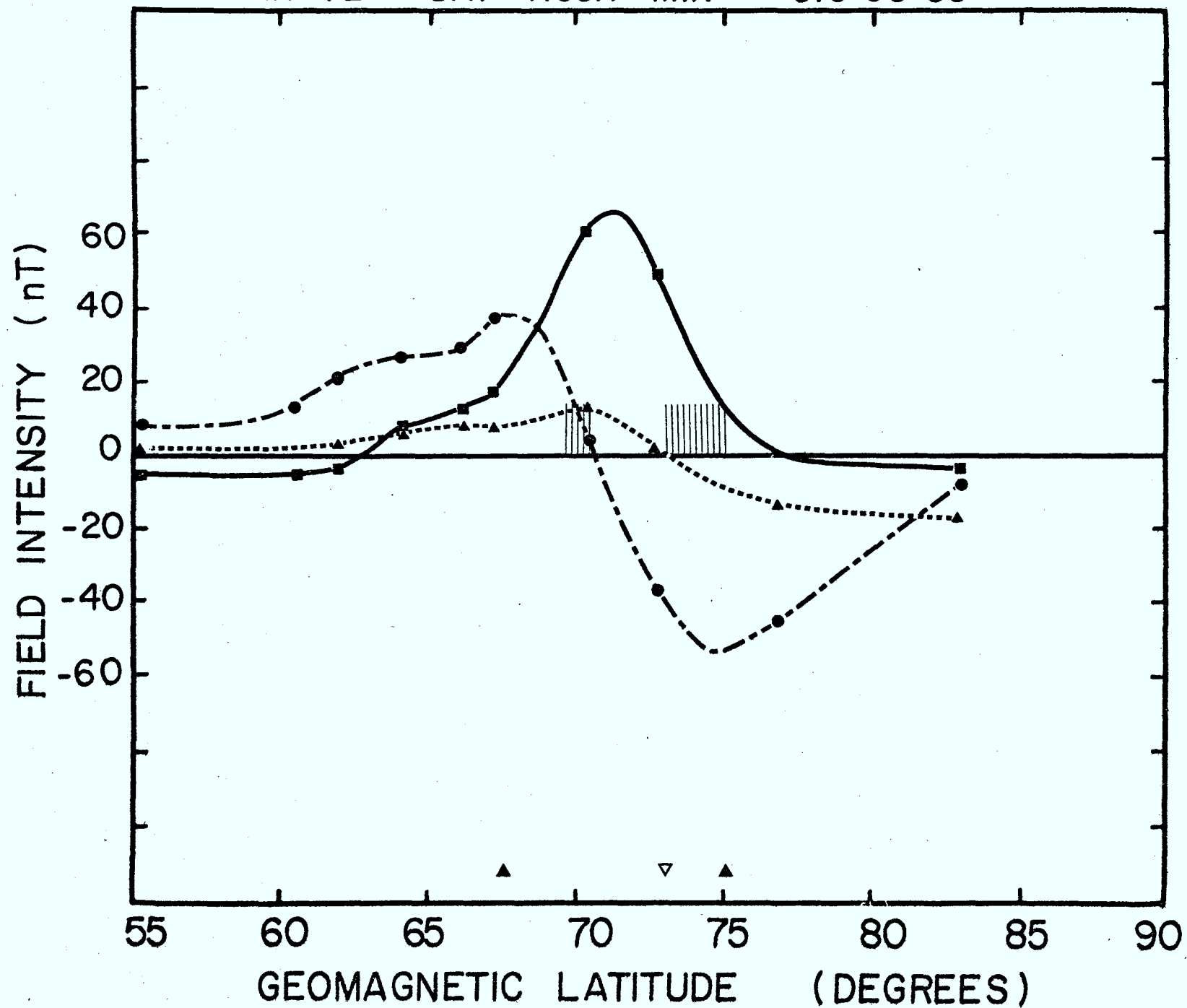
YEAR 72   DAY: HOUR: MIN.   010:03:35

Figure 11: Same as Figure 4 except for Day 10, 1972 at 0335 UT.

bar shows the region of noise with amplitude greater than -70 db. The noise spectra are shown in Figure 12. Auroral data were available from Wallis et al. and the diffuse aurora was observed in the latitude range $66° < \Lambda < 77°N$. The energetic electron spectrogram from the SPS is shown in Figure 13.

Again, as in the two previous cases, the noise level builds up as the satellite approaches the poleward border of the eastward electrojet. In this case an auroral arc is situated approximately at the poleward border of the eastward electrojet, and there is an intense flux of energetic electrons (with energies up to ~ 4 keV) and strong noise at this location. The satellite passes through some structured arcs in the latitude range 71-73°N, where the electron fluxes have energies reaching ~ 1 keV. The noise in this latitude range is somewhat reduced; this is perhaps related to the drop in the peak energy of the electrons, and would agree with a similar observation made for Case 2. The region from $\sim 67.5 - 71°N$ is dominated by energetic electron fluxes with peak energies between 5-10 keV; an auroral arc centered at $\sim 68.5°N$ sits in this region, however the noise amplitudes are rather low (with the exception of a brief secondary enhancement at $\sim 70°N$, which is typical of the two previous cases). Clearly the presence of fluxes of energetic electrons in the energy range > 1 keV does not necessitate the production of noise. It may well be that both the presence of such energies in the electron spectrum and a positive gradient in velocity space are necessary to ensure the production of noise.

Again, the equatorward portion of the electrojet is devoid of noise, despite the presence of an auroral arc just north of 68°N. It should be noted that the equatorward border of the electrojet in this case is somewhat more difficult to define, since the ΔZ profile is rather irregular and there
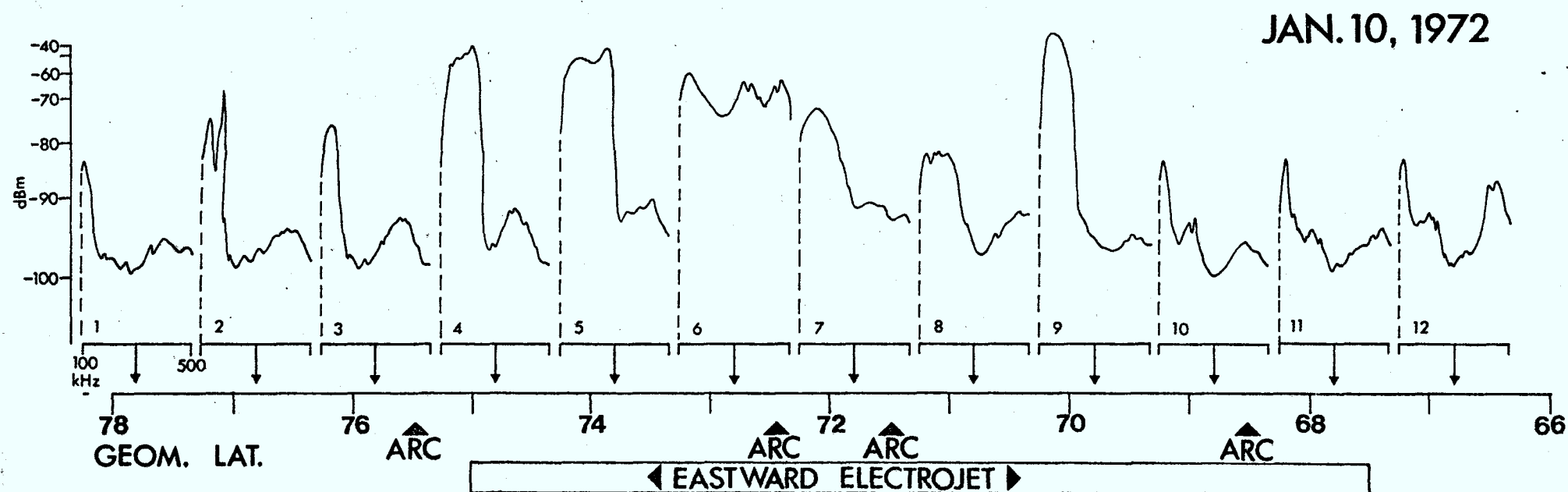
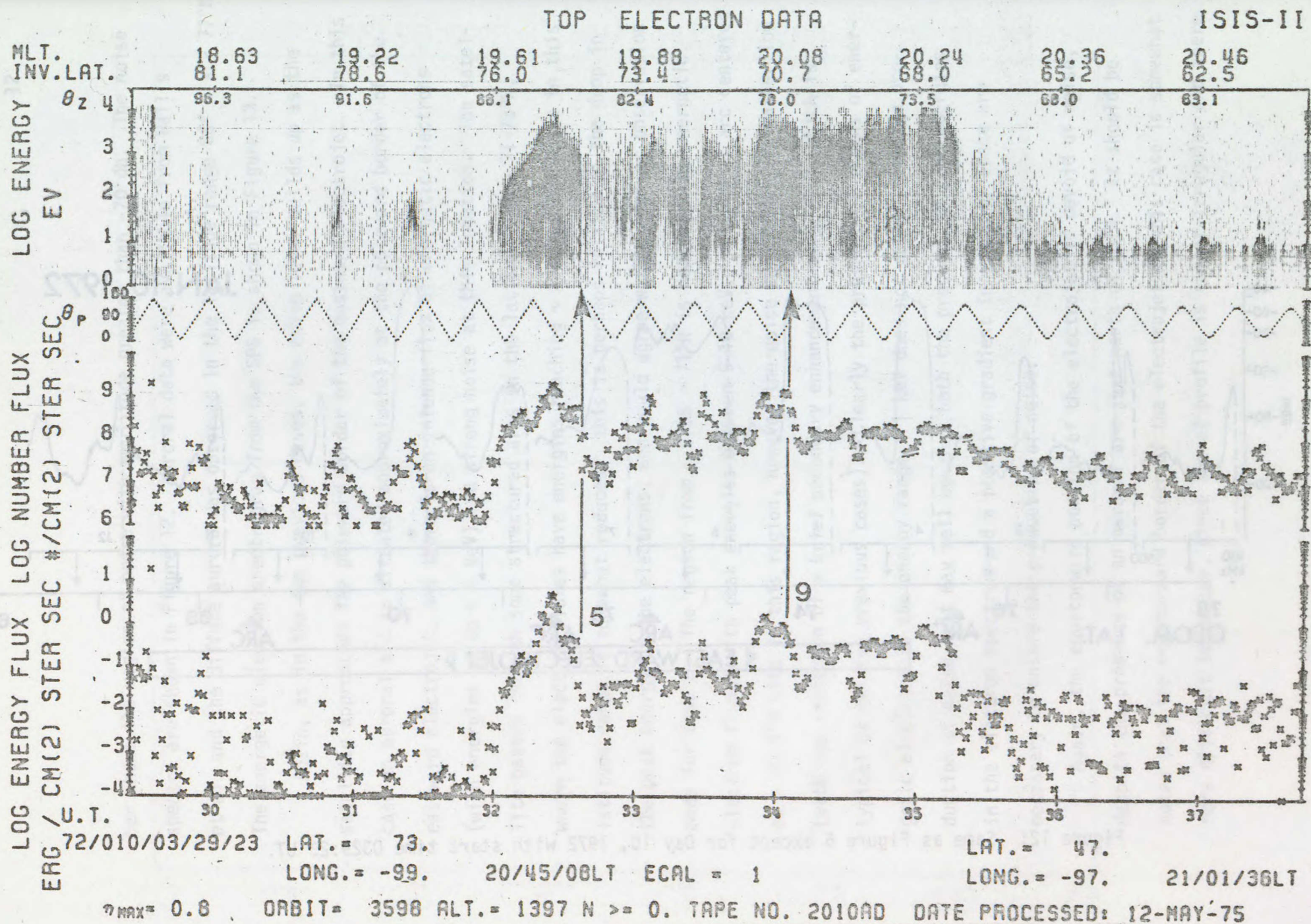Figure 12: Same as Figure 5 except for Day 10, 1972 with start time 0329:23 UT.

Figure 13: Same as Figure 6 except for Day 10, 1972 with start time 0329:23 UT.

are two possible explanations for the irregularity. If the $+\Delta Z$ in the latitude range 60-67°N is due to the end effect of the S_q^p current system whose currents are, in part, diverted up magnetic lines of force at the conductivity discontinuity marked by the dusk terminator (Rostoker et al., 1977), then the identification of the equatorward boundary of the electrojet associated with the auroral luminosity is correct as stands. If however, the irregular behaviour of ΔZ is due to the fact that the current is nonuniformly distributed across the electrojet (viz. the current is more intense at the poleward border), Kisabeth (1972) has shown that the equatorward border of the electrojet could be as low as $\sim$ 62°N.

Case 4   Eastward Electrojet in the Evening Sector with a

        Weak Westward Electrojet to the North

        Day 11, 1972   Start time 0408 UT

The satellite was on a southbound pass along geographic meridian $\sim$ 109°W ($\sim$ 2° to the east of the station line). The topside sounder aboard the satellite was in the fast sweep mode. The latitude profile of the ground magnetic perturbations at 0413 UT is shown in Figure 14, and indicates an eastward electrojet in the latitude range 64 < Λ < 74°N with a maximum perturbation of $\sim$ 120 nT. The $+\Delta Z$ at the most poleward station suggests the existence of a westward electrojet poleward of 74°N. The profile was relatively stable over the interval of the pass, although the pass took place during relatively a high level of activity (K_p = 4-). The shaded bar again indicates the region of noise with amplitude greater than -70 db; the noise spectra are shown in Figure 15 and the energetic electron data are shown in Figure 16. Again, data from the paper of Wallis et al. revealed
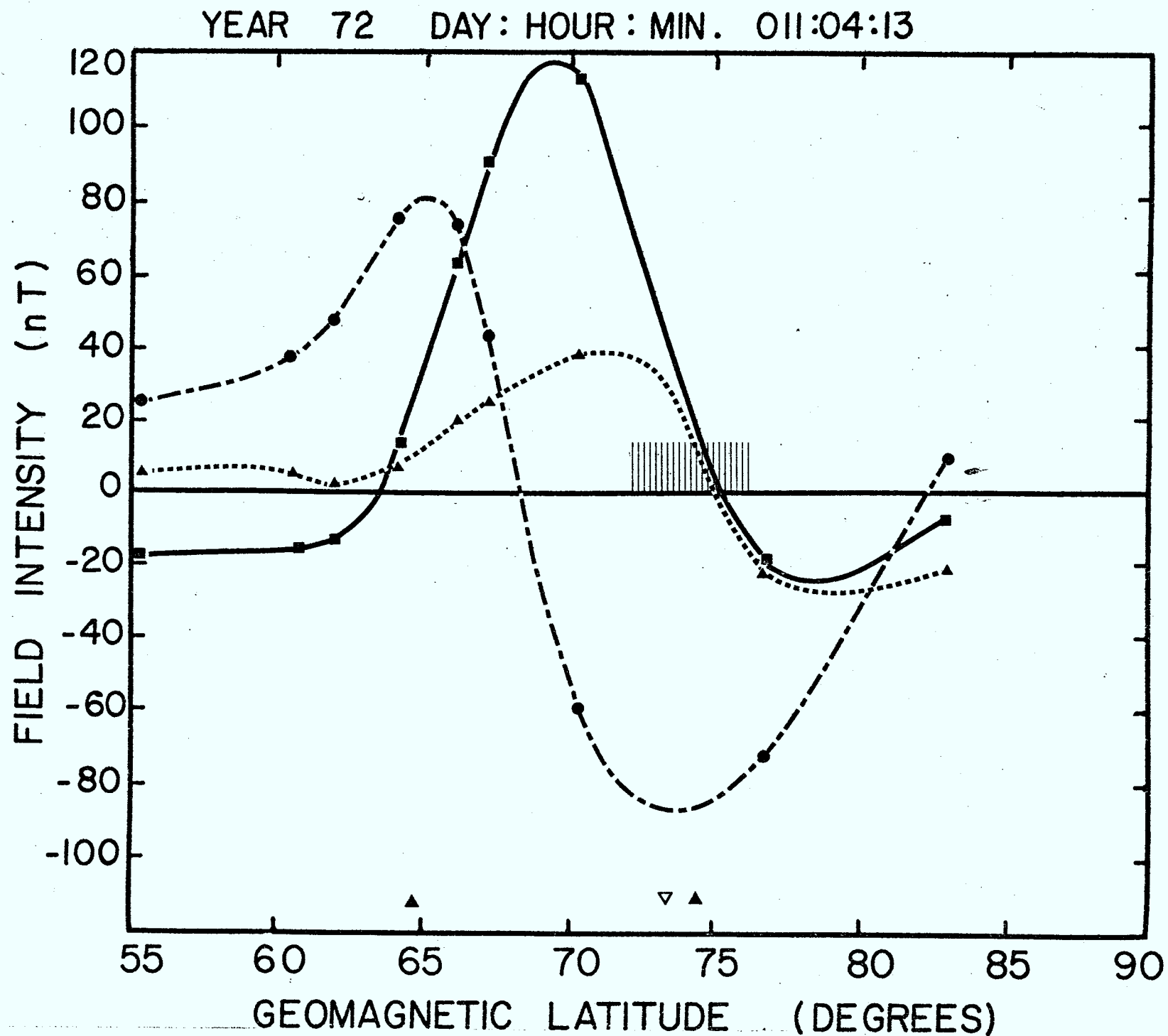
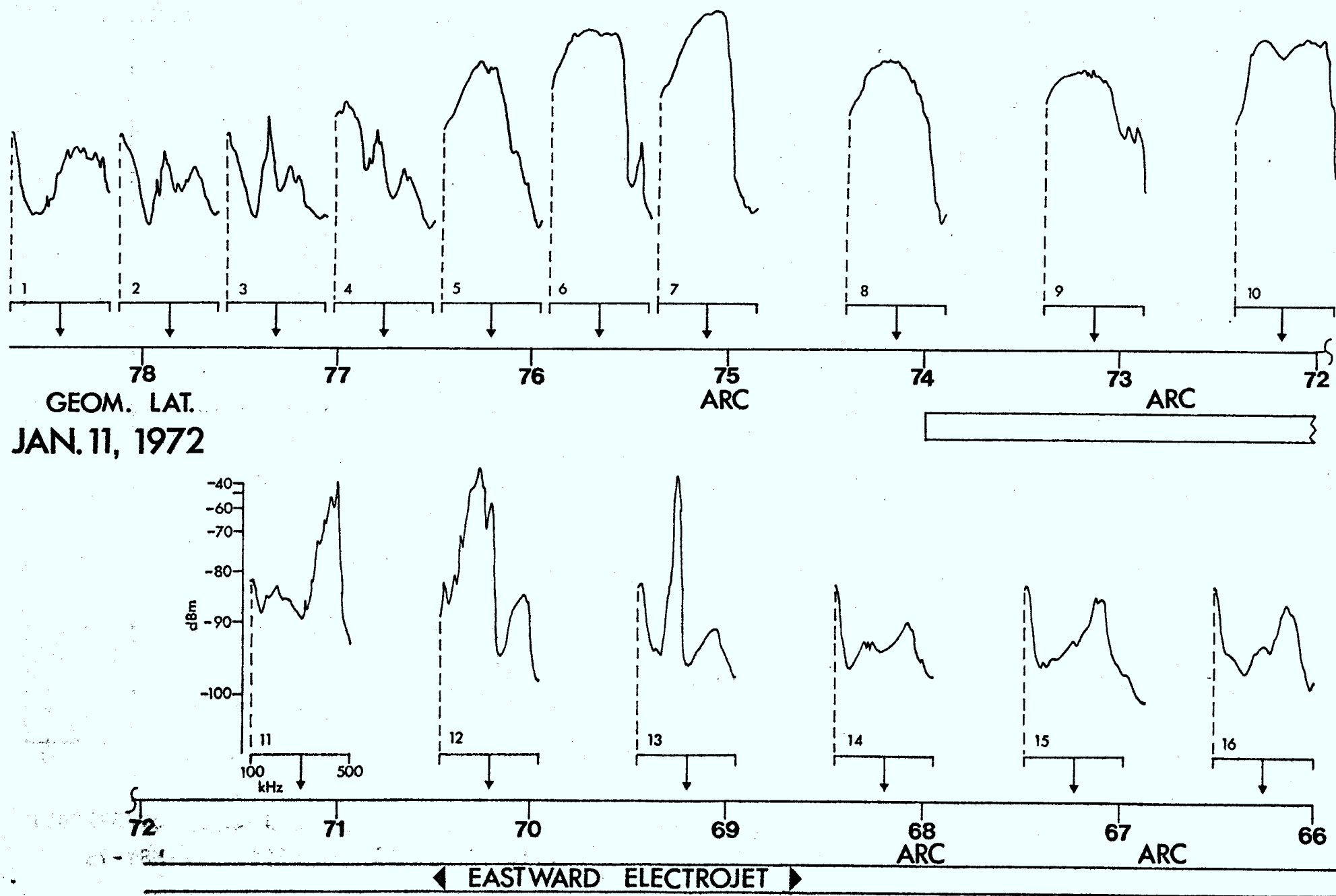Figure 14: Same as Figure 4 except for Day 11, 1972 at 0413 UT.

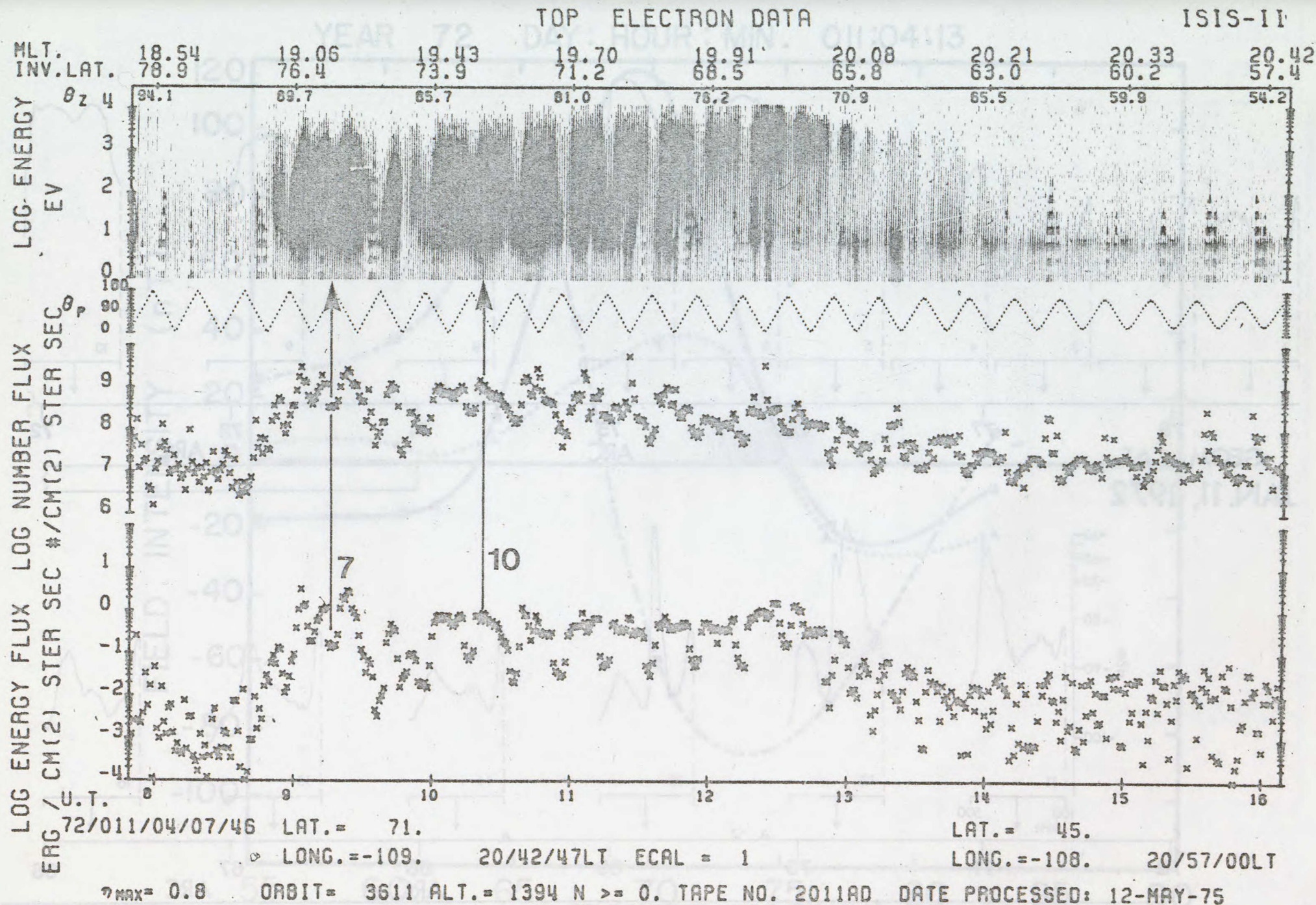Figure 15: Same as Figure 5 except for Day 11, 1972 with start time 0407:46 UT.

Figure 16: Same as Figure 6 except for Day 11, 1972 with start time 0407:46 UT.

a diffuse auroral oval extending over the region 63 < Λ < 77°N with discrete arcs centered at latitudes of ∿ 75-76°N, 72-73°N, 68°N and 67°N.

Again the satellite encountered a buildup in noise level as it approached the poleward border of the eastward electrojet. However, in this case high noise levels rich in the higher frequencies (f > 200 kHz) were encountered north of the poleward border of the eastward electrojet. This region of enhanced noise coincided with strong fluxes of energetic electrons whose peak energies ranged from ∿ 1-3 keV. This, therefore is a region of noise and auroral luminosity in the form of an arc which appears to coincide with some westward ionospheric current flow. At the predicted position of the poleward boundary of the eastward electrojet, there is a marked decrease in energy flux and the peak energy of the electrons drops below 1 keV; associated with this dropout in the more energetic electrons, there is a noticeable decrease in the amplitude of the noise. The noise level builds up again towards 72°N where a second auroral arc is identified; in this region, again peak electron energies exceed 1 keV. Equatorward of 72°N the noise becomes markedly less intense and more erratic, effectively disappearing equatorward of ∿ 69°N near the center of the eastward electrojet. Even though strong fluxes of energetic electrons extend down to ∿ 66°N, and two arcs are observed near 67° and 68°N, the noise is clearly absent indicating that energetic electron fluxes with peak energies greater than 1 keV and enhanced auroral luminosity are apparently necessary but not sufficient conditions for noise generation. These conclusions confirm those reached in Case 3.

Case 5   Eastward electrojet in the Evening Sector With a

          Westward Electrojet to the North

          Day 17, 1972   Start time 0406 UT

The satellite was on a southbound pass along geographic meridian 115°W
($\sim$ 4° west of the station line). The topside sounder was in the fast sweep
mode. The latitude profile of the magnetic perturbation pattern, shown in
Figure 17, indicates a strong rather narrow eastward electrojet in the lat-
itude range 62 < Λ < 67°N with a maximum perturbation of $\sim$ 150 nT. There
was a rather broad region of westward current flow north of the eastward
electrojet; the general level of activity during this period was rather
high (K_p = 40). The noise above -70 db in amplitude is indicated by the
shaded bar in Figure 17, while the noise spectra themselves are shown in
Figure 18 and the SPS electron data in Figure 19.

The region poleward of the northern border of the eastward electrojet
is filled with noise in the frequency range 100 < f < 200 kHz up to 72-73°N.
This poleward boundary is precisely that assigned by Wallis et al. to the
poleward boundary of the auroral oval (the equatorward boundary being set
$\sim$ 62°N). As the satellite moves equatorward it encounters an arc at 69-70°N,
in which range the noise has a markedly higher frequency content (spectra
6 and 7). The SPS indicates enhanced electron fluxes equatorward of $\sim$ 73°N
when it crosses the poleward border of the auroral oval. It is interesting
to note that the "burst" of electrons at 73°N has peak energies of < 1 keV,
no identifiable auroral arc and no high frequency (f > 200 kHz) noise con-
tact (although lower frequency noise appears to be enhanced at that boundary).

There is a noticeable drop in noise level near the poleward boundary
of the eastward electrojet, which appears to coincide with a drop in peak
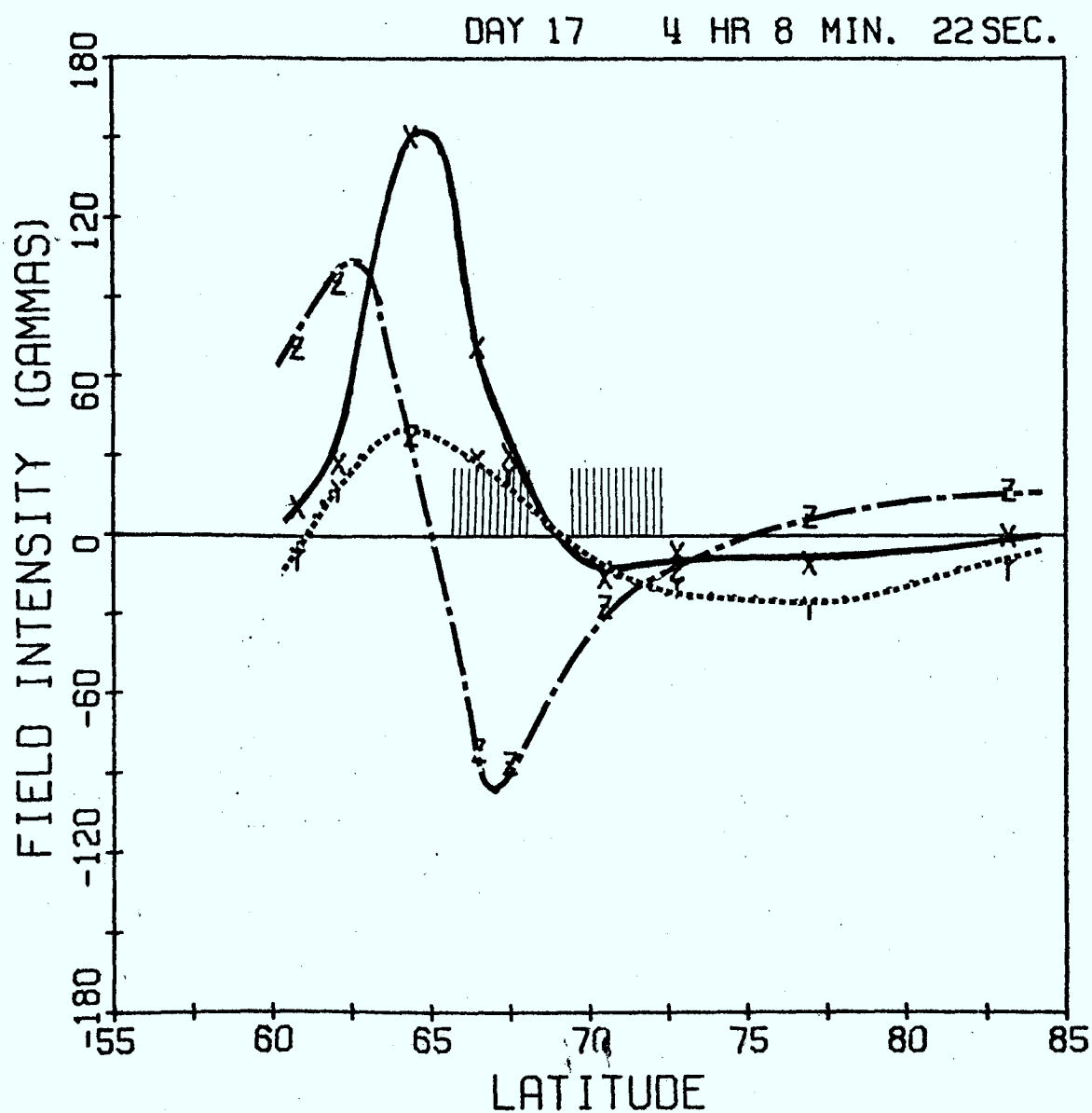
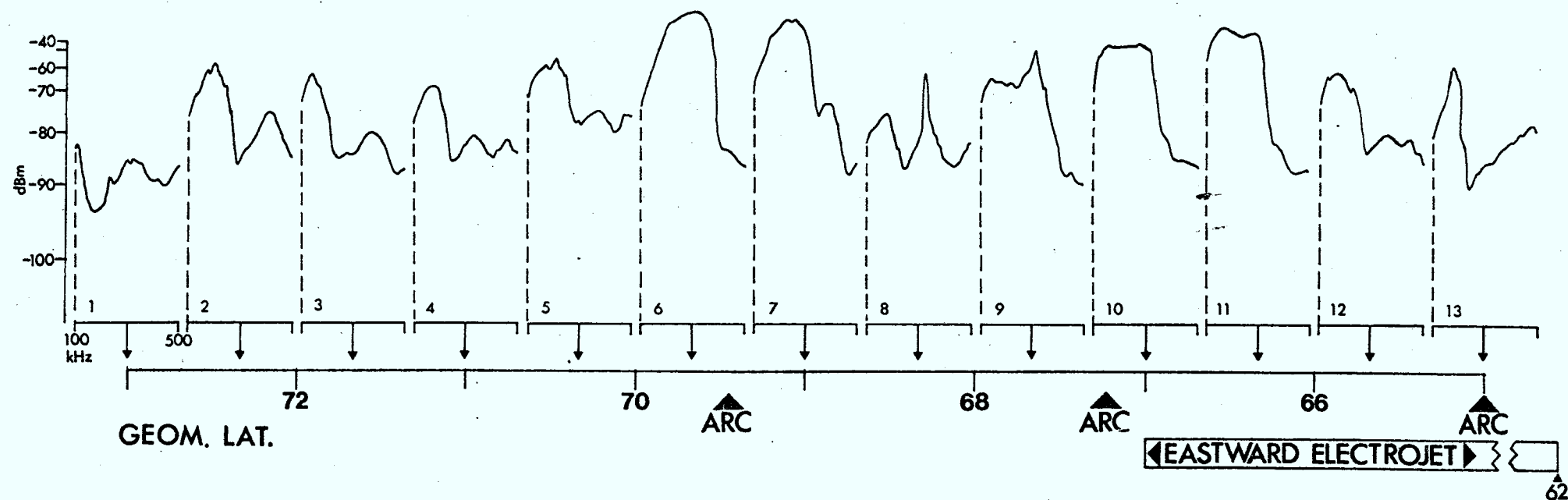Figure 17: Same as Figure 4 except for Day 17, 1972 at 0408 UT.

JAN. 17, 1972

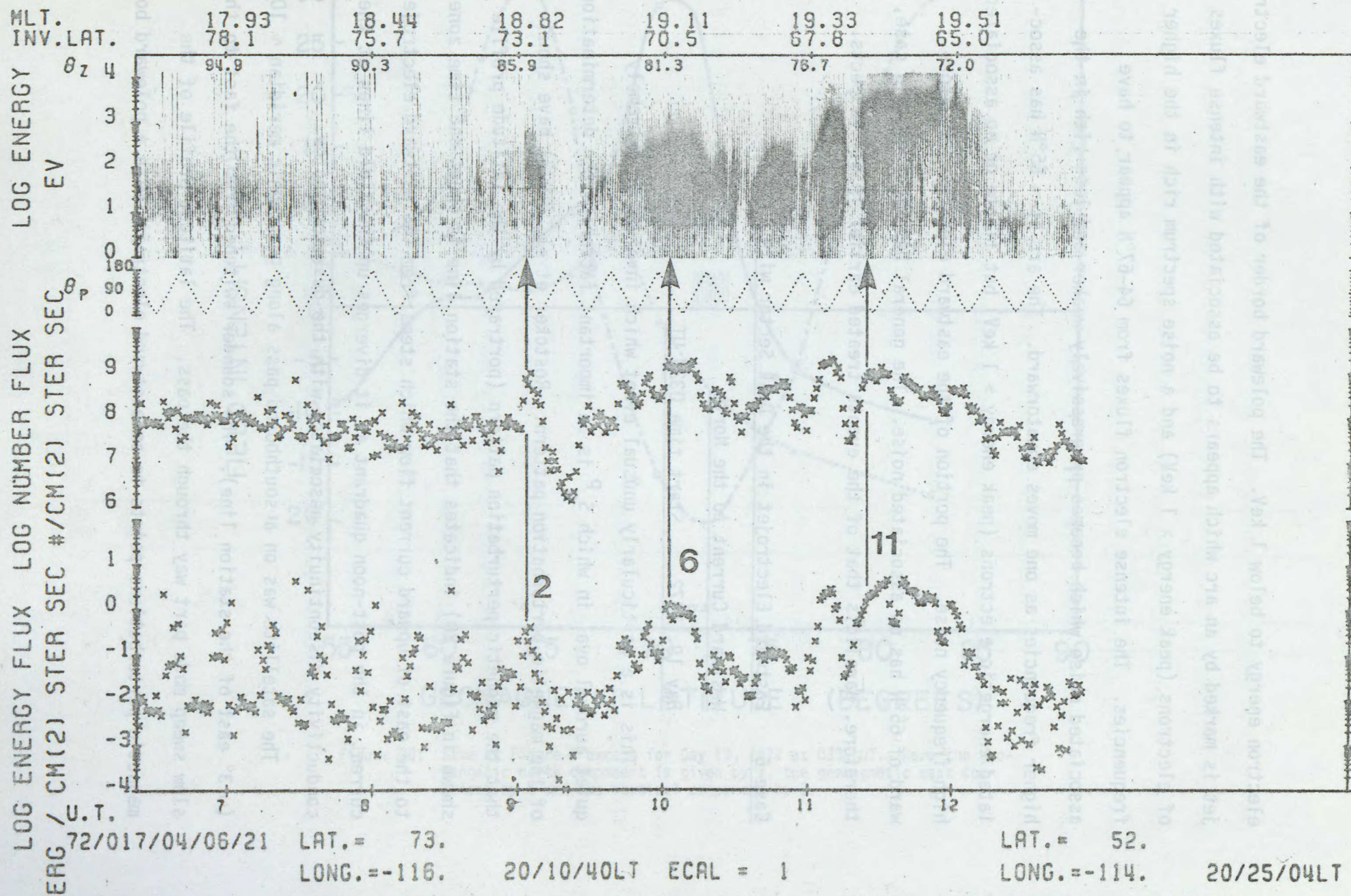Figure 18:   Same as Figure 5 except for Day 17, 1972 with start time 0406:21 UT.

Figure 19: Same as Figure 6 except for Day 17, 1972 with start time 0406:21 UT.

electron energy to below 1 keV. The poleward border of the eastward electro-
jet is marked by an arc which appears to be associated with intense fluxes
of electrons (peak energy > 1 keV) and a noise spectrum rich in the higher
frequencies. The intense electron fluxes from 64-67°N appear to have
associated noise which becomes progressively weaker and less rich in the
higher frequencies as one moves equatorward. The arc at $\sim$ 65°N has assoc-
iated energetic electrons (peak energy > 1 keV) but little or no associated
high frequency noise. The portion of the eastward electrojet equator-
ward of 65°N has no associated noise. The general behaviour of this case,
therefore, parallels that of the events treated earlier in all respects.

Case 6   Eastward Electrojet in the Dusk Sector with
          Westward Current to the North
          Day 19, 1972   Start time 0329 UT

This is a particularly unusual event which involves an extremely
quiet auroral oval in which S_q^p is an important factor in the determination
of the magnetic perturbation pattern. Rostoker et al. (1977) have shown
that the magnetic perturbation pattern (portrayed by the latitude profile
shown in Figure 20) indicates that the station line is about one time zone
to the east of upward current flow which stems from the eastward electrojet
current in the post-noon quadrant as it diverges up the field lines at the
conductivity discontinuity associated with the dusk terminator.

The satellite was on a southbound pass along geographic meridian $\sim$ 108°W
($\sim$ 3° east of the station line). The sounder switched from the fast to the
slow sweep mode part way through the pass. The latitude profile of the
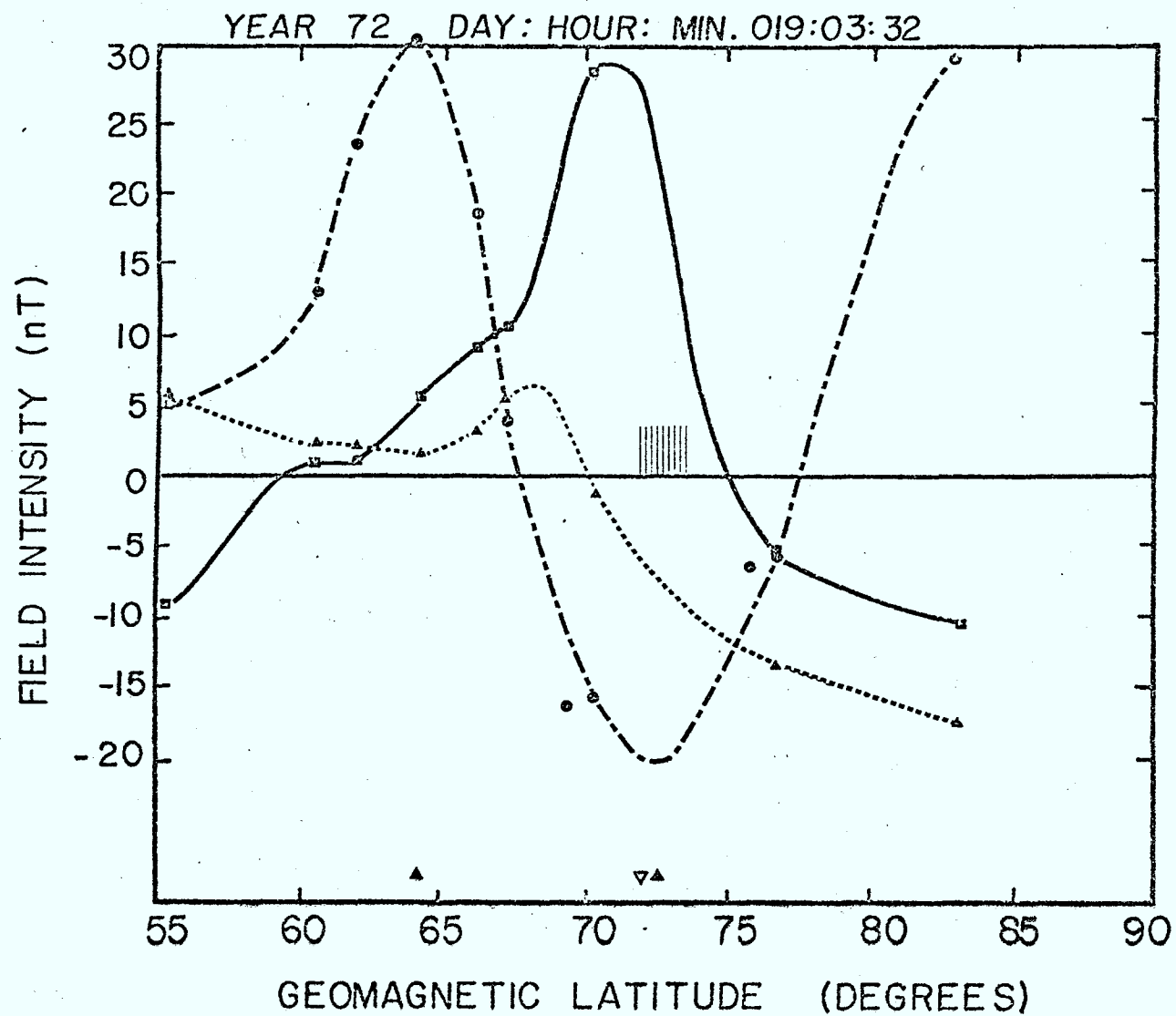magnetic perturbations points to an eastward electrojet with a poleward border

Figure 20: Same as Figure 4 except for Day 19, 1972 at 0332 UT. Here the geo-
mangetic north component is given by X, the geomagnetic east com-
ponent by Y and the vertical component by Z.

near $\sim$ 73-74°N and an equatorward border near $\sim$ 68-69°N. [The large +ΔZ
at low latitude is thought to be the edge effect of the eastward electrojet's
associated north-south Pedersen current and Birkeland current sheets at the
conductivity discontinuity which exists at the dusk terminator.] The electro-
jet magnitude is rather weak (peak amplitude being $\sim$ 30 nT), and the system
was stable over the interval of the pass. Positive ΔZ and negative ΔH to
the north indicate westward current flow poleward of the eastward electrojet.
The shaded bar in Figure 20 indicates the region of noise with amplitude
greater than -70 db; the noise spectra are shown in Figure 21 and the SPS
electron data in Figure 22.

As in all previous cases, the lower frequency noise (100 < f < 200 kHz)
builds in amplitude as the satellite approaches the poleward border of the
eastward electrojet. At the poleward border there is a marked enhancement
of energetic electron fluxes with peak energies exceeding $\sim$ 5 keV. Al-
though the sweep rate unfortunately changed from fast to slow mode at this
time, spectrum 6 (Figure 21) clearly shows enhanced amplitude and a richer
high frequency portion of the noise spectrum in the region of enhanced keV
electron fluxes. [Although auroral data were not available for this pass,
we would predict a discrete auroral arc or group of arcs in the latitude
range 72-73°N.] The equatorward portion of the electrojet in the latitude
range 68 < Λ < 72°N featured no significant noise although there were
energetic electron fluxes with peak energies greater than 1 keV.
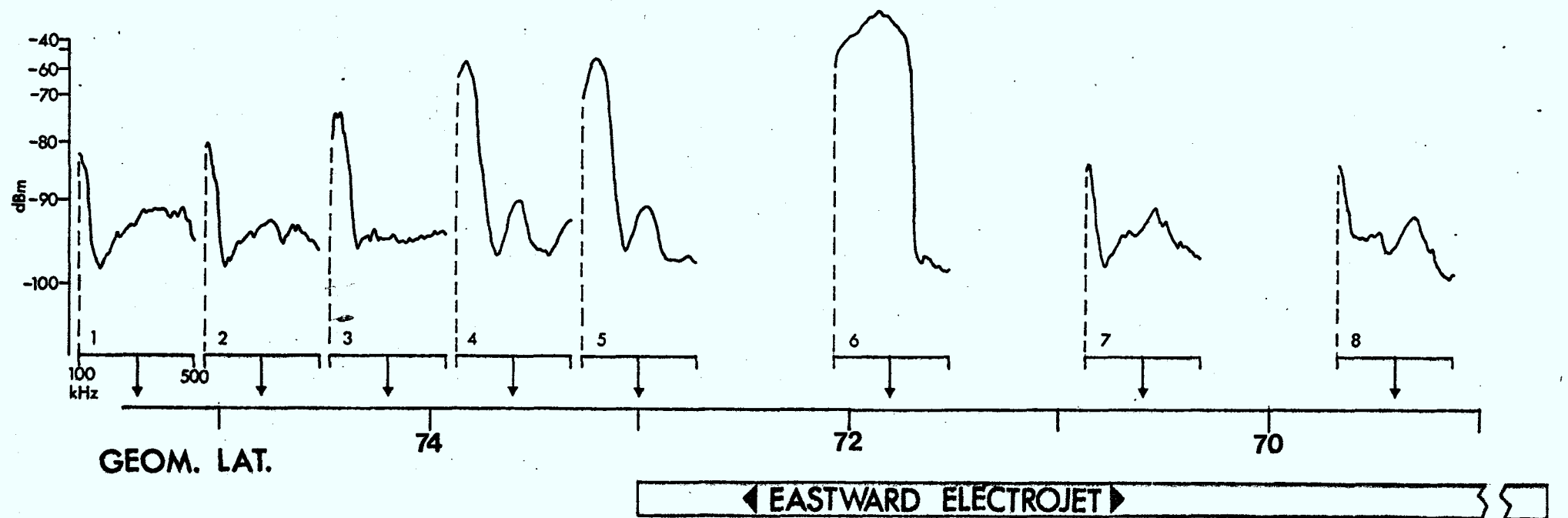
Figure 21: Same as Figure 5 except for Day 19, 1972, with start time 0328:27 UT.

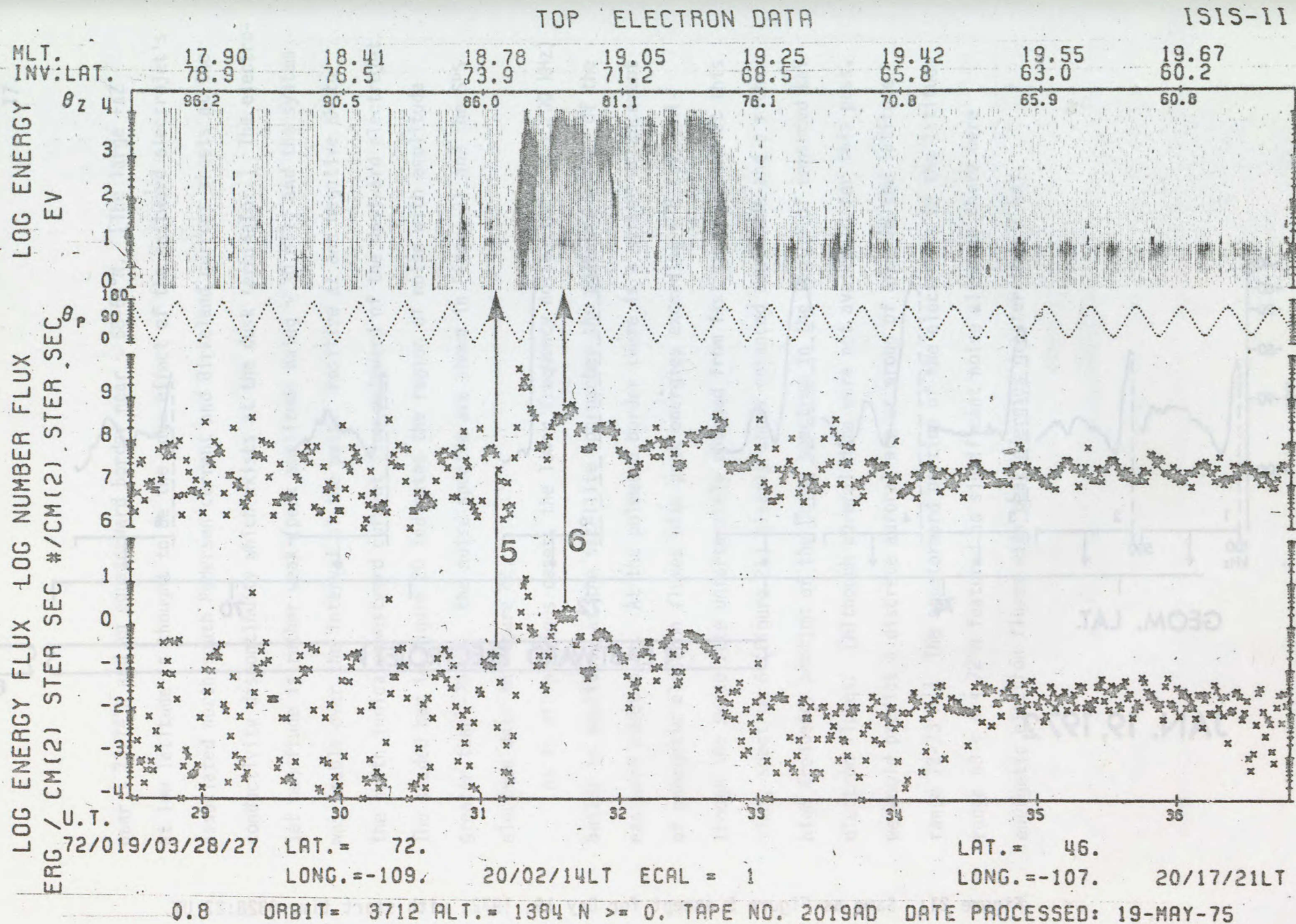Figure 22: Same as Figure 6 except for Day 19, 1972 with start time 0328:27 UT.

Case 7   Substorm Westward Electrojet in the Evening Sector

Day 360, 1971   Start time 0525 UT

It is not common to have the opportunity to study polar orbiter data when the satellite is known to have passed through a substorm disturbed region in the heart of the expansion phase. This pass yielded the possibility of carrying out just such a study.

The satellite was again on a southbound pass along geographic meridian ∿ 110°W (∿ 1° east of the station line). The topside sounder was in the fast sweep mode, however, unfortunately no data were received equatorward of ∿ 63°N. Nonetheless, most of the dynamic activity was concentrated near the poleward border of the substorm disturbed region so there was much to learn from this event.

The latitude profiles during the interval of the pass showed rapid magnetic variations of large magnitude, as one might expect during a substorm expansion phase. Figure 23 shows a profile near the time of the satellite passage over the poleward portion of the electrojet. A study of other auroral zone and low latitude magnetograms in the North American sector reveal that the substorm sequence (Wiens and Rostoker, 1975) was initiated in eastern North America prior to 0500 UT, and entered the longitudinal region of the Alberta station line ∿ 0510 UT. The peak disturbance occurred approximately at the time of the ISIS pass. The latitude profile in Figure 23 reveals a strong westward electrojet with a double peak; this is indicative of a strong westward electrojet with equatorward border near ∿ 64°N with an intense poleward segment whose poleward edge lies near ∿ 73.5°N. Peak magnetic perturbations across the electrojet region reach ∿ 500 nT. The shaded bar in Figure 23 again indicates the region of noise with amplitude
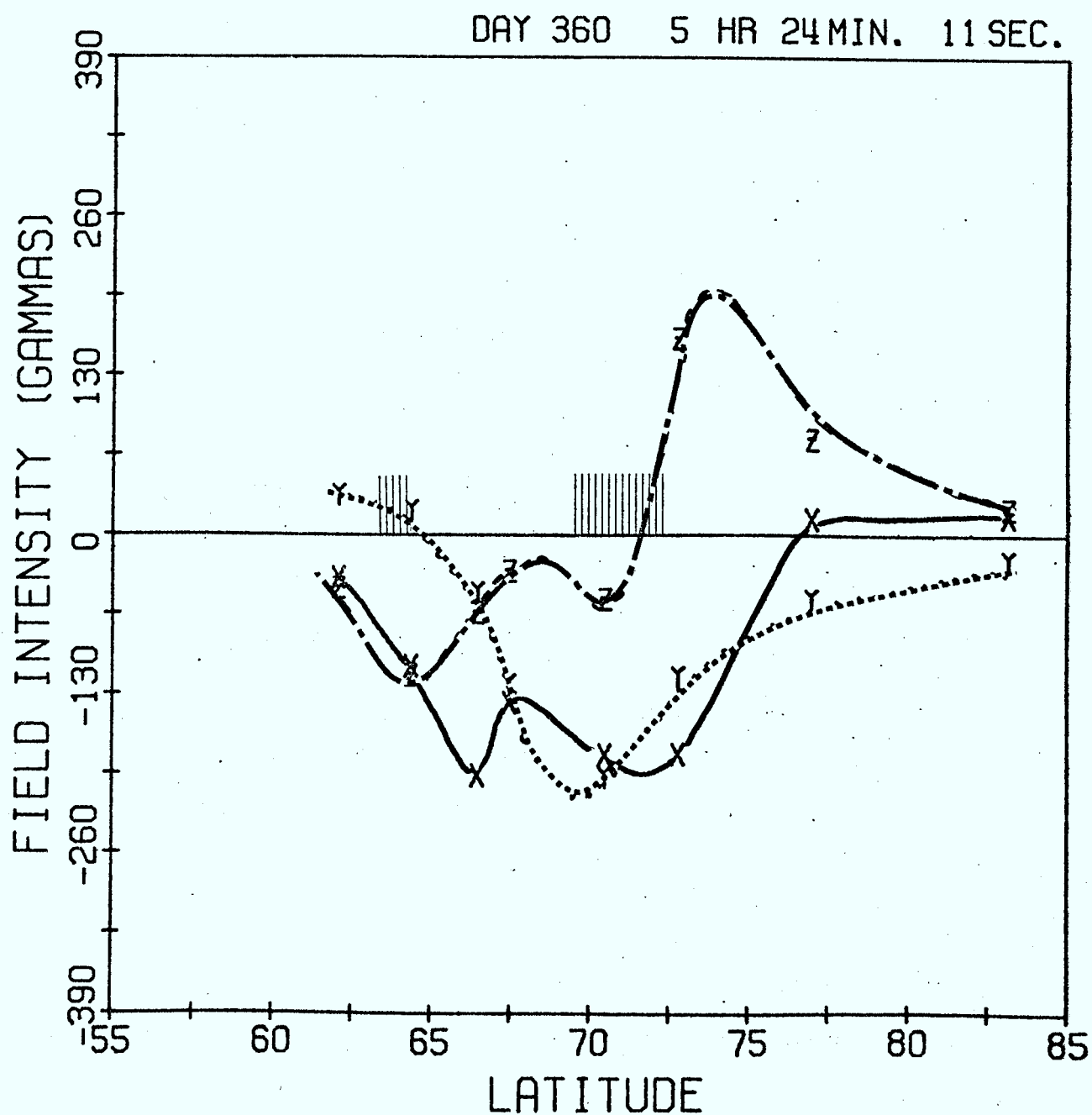
Figure 23: Same as Figure 20 except for Day 360, 1972 at 0524 UT.

greater than -70 db; the noise spectra are shown in Figure 24 and the SPS electron data appear in Figure 25.

As the satellite moved equatorward from the polar cap, a slight increase in noise level was observed at the predicted poleward border of the substorm westward electrojet $\sim$ 73-74°N (spectra 4 and 5 in Figure 24) but the most intense noise was not encountered until the satellite was well within the borders of the westward electrojet. At this time, the SPS electron spectrogram (Figure 25, arrow 7) shows a small enhancement of electrons with energies of $\sim$ 1 keV and below. Further south, in the latitude range 69° < Λ < 71.5°N, a large flux of 1 to 8 keV electrons is found to correlate with intense noise with an upper frequency cutoff of $\sim$ 300 kHz. It is interesting to note, however, that in the region north of 71.5°N there is an absence of energetic electrons even though the noise is still quite strong (see spectra 7 and 8). Since substorm current systems are known to be confined at times to rather narrow longitudinal sectors, one might expect that the noise could be coming from a source region slightly to the east of the satellite subtrack. In this case the particle detectors would not necessarily encounter the energetic electrons responsible for the generation of the observed noise. In addition the magnetometer line would observe the profile shown in Figure 23 even if it were off the edge of an intense substorm westward electrojet element; thus, for substorm events where short electrojet elements are not atypical, such ambiguities can exist in identification of overhead current flow.

Centered at $\sim$ 67°N is less intense noise associated with the observed flux of electrons ranging in energies up to $\sim$ 4 keV (see Figure 25 arrows 14 and 15). The only noise associated with the enhanced current flow in

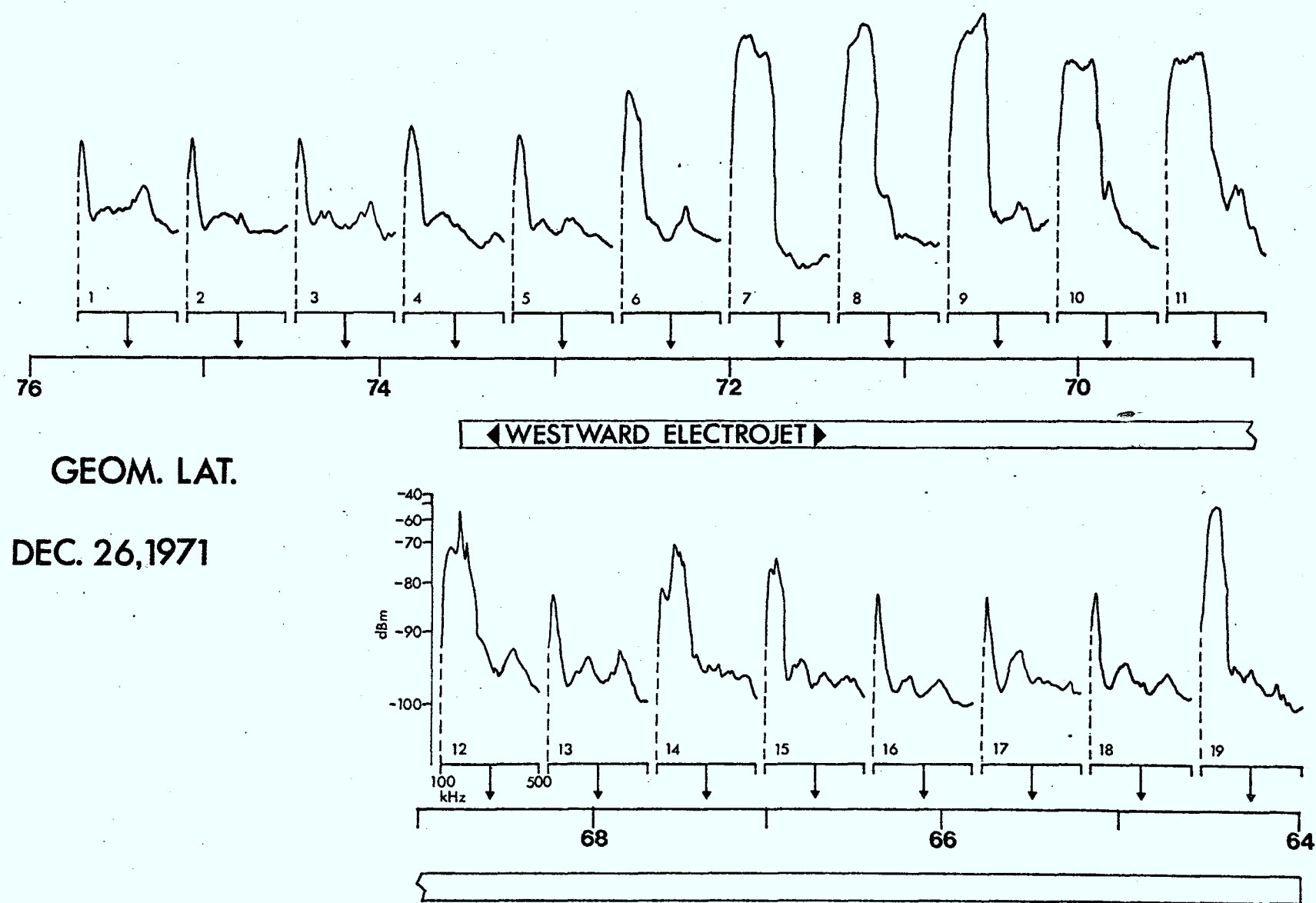GEOM. LAT.

DEC. 26,1971

WESTWARD ELECTROJET

Figure 24: Same as Figure 5 except for Day 360, 1972 with start time 0525:22 UT.

the southern part of the electrojet (see Figure 23) occurred between 64° and 65°N. At this position, the electron spectrogram shows a number flux enhancement of low energy electrons (∿ 100 eV and below). Again, one must be careful in the identification of the source region since the southern part of the current system was fairly active during this event. More intense source regions east and west of the satellite could also exist. In this respect it is worth pointing out that the intense fluxes of low energy (E ≤ 100 eV) electrons equatorward of 64°N have no associated noise (the noise profiles are not shown here). Thus, either some low energy fluxes are associated with noise and others are not, or indeed the longitude of the source region with respect to the satellite subtrack must be considered.

Discussion of the Data

(i) Phenomenology of the noise distribution

We begin our discussion by studying the bar chart shown in Figure 3 to ascertain the relationship between the noise measured aboard the satellite at 1400 km and the current carrying ionospheric electrojet regions. The following conclusions, supported by the more detailed case studies, are as follows:

(1) Noise is absent in the equatorial portions of eastward electrojets.

(2) All eastward electrojets have noise in their poleward portions and poleward of their northern borders.

(3) All westward electrojets in the evening sector have associated noise.

(4) There is no apparent correlation between noise and thermal plasma enhancements at 1400 km.
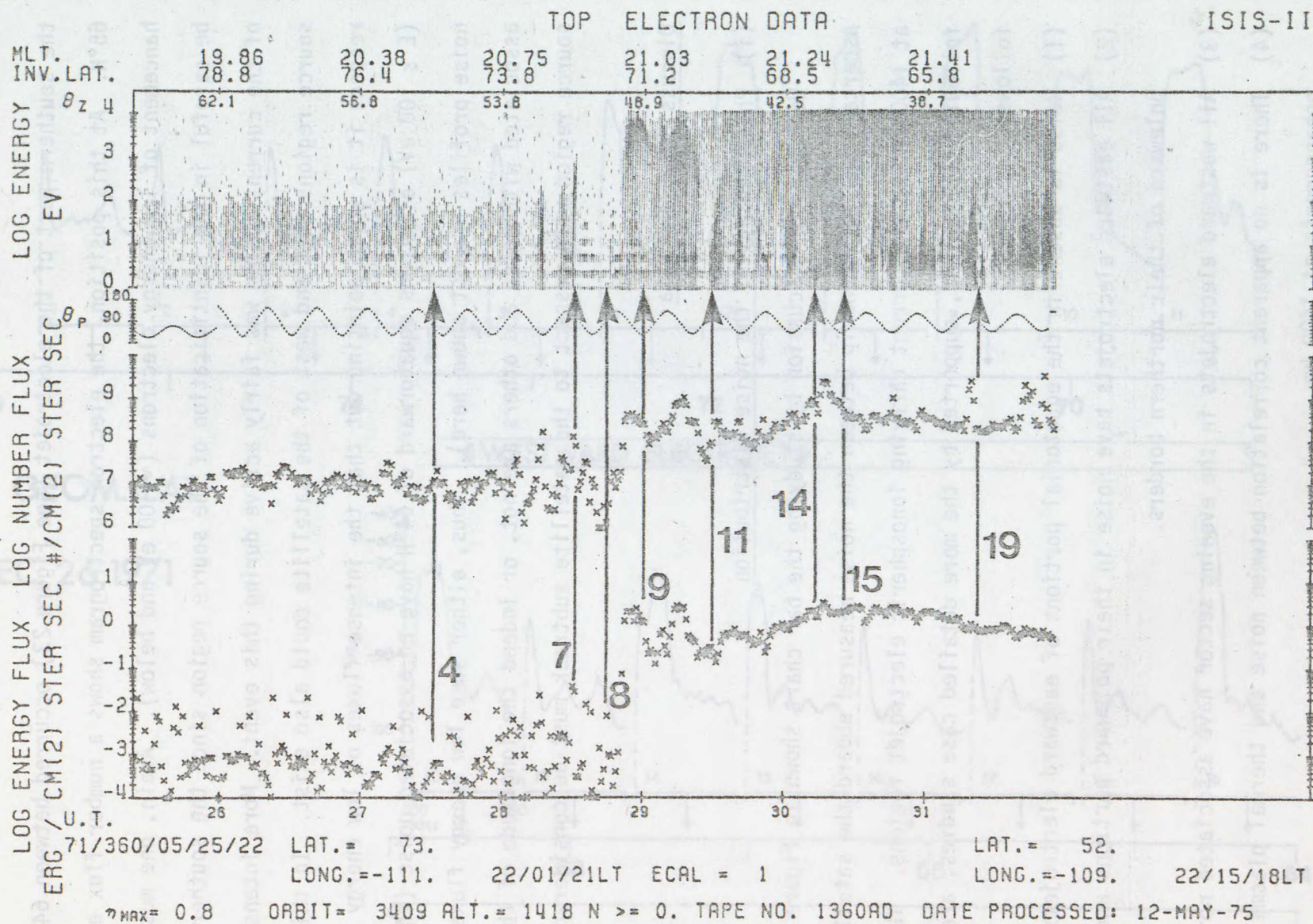
Figure 25: Same as Figure 6 except for Day 360, 1972 with start time 0525:22 UT.

These general observations can be supplemented by additional conclusions reached using the more detailed correlated data (auroral luminosity and energetic electron fluxes) presented in the case studies. Then additional conclusions are as follows:

(5) Low frequency (f < ∿ 200 kHz) noise may be observed outside the region of energetic electron fluxes or in regions where peak energies are below 1 keV in the poleward portion of the electrojet. Low amplitude low frequency noise may be detected above the equatorward portion of the electrojet.

(6) High frequency noise (f < ∿ 200 kHz) appears only in regions where the peak energy of the energetic electron flux exceeds ∿ 1 keV and where discrete auroral arcs are identifiable in the poleward portion or poleward of the eastward electrojet in the evening sector.

(7) The center of an auroral arc appears to be the site of the highest noise frequencies and amplitudes. The high frequency content decreases as one moves away on either side of the auroral arc as shown schematically in Figure 26.

We shall now explore the relationship between auroral arcs, energetic electrons and noise in more detail. First we note that it is becoming increasingly apparent that auroral arcs in the poleward region of the auroral oval are associated with 'inverted-V' structures in electron energy spectrograms reported by Frank and Ackerson (1972) and Ackerson and Frank (1972). These structures were proposed by Gurnett (1972) to be the site of electric potential configurations such as that shown in Figure 27. Therefore the 'inverted-V's' also are associated with an electric field reversal and with
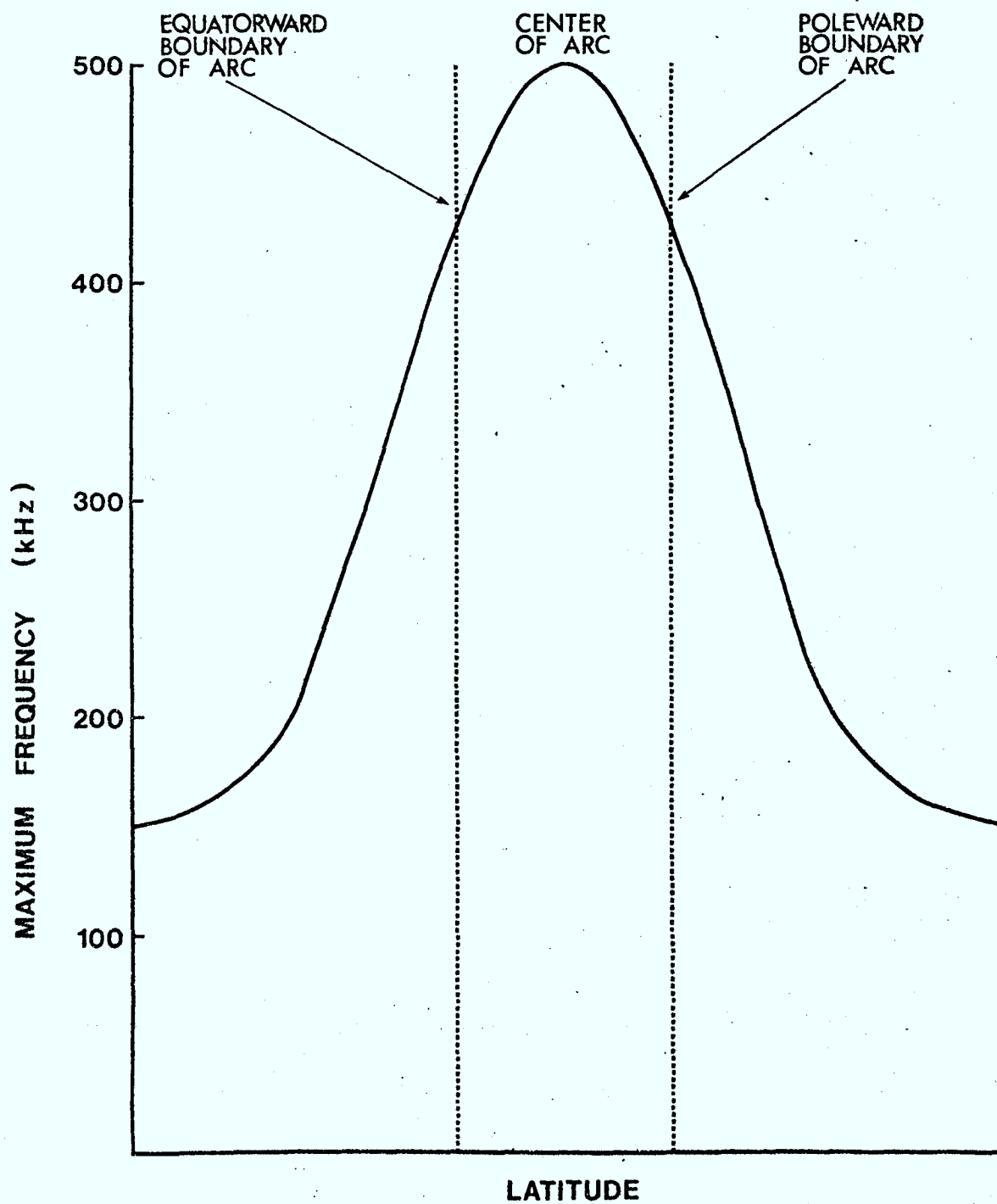
Figure 26: Schematic diagram showing the variation of the maximum frequency of noise in the frequency range 100 < f < 500 kHz across the region of an auroral arc.
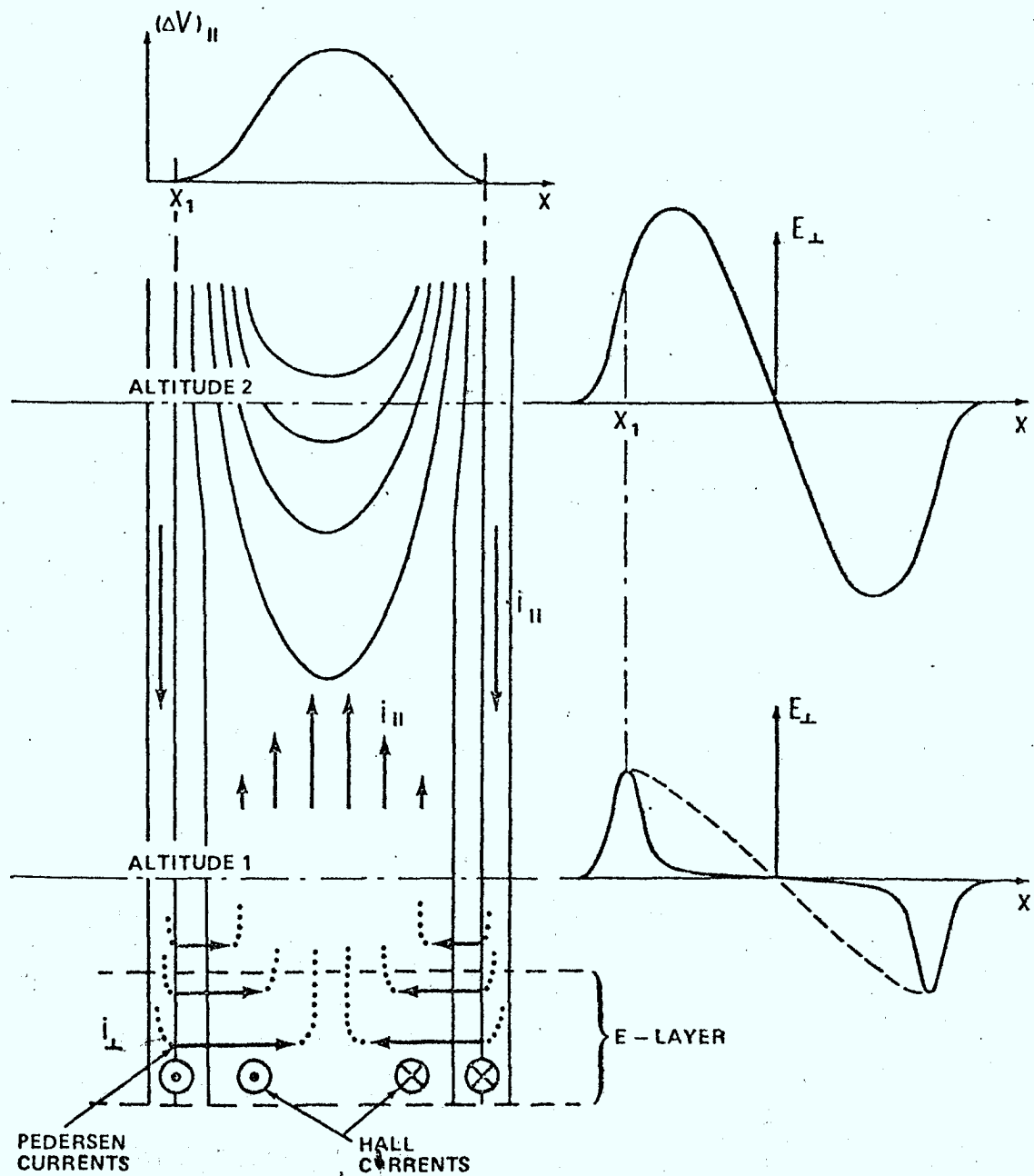
Figure 27: Electric potential distribution associated with an auroral arc (after Burch et al., 1976). Note the change in horizontal electric field configuration with altitude associated with the potential drop parallel to magnetic lines of force.

downward field-aligned currents at the edges and upward field-aligned currents at the center of the structure. Burrows (1974) and Winningham et al. (1975) have discussed the energetic particle precipitation patterns in the evening sector in some detail. Both tend to regard the regions of the plasma sheet mapping to the poleward and equatorward portions of the evening sector auroral oval as different entities. Winningham et al. (1975) have termed the poleward portion the boundary plasma sheet (bps) and the equatorward portion the central plasma sheet (cps). The phenomenology of these regions can be understood as follows. Electrons in the bps region are relatively freshly injected into the plasma sheet and are in the process of being accelerated. There is every indication that the acceleration processes are at rather low altitude, and parallel electric fields which are good candidates for the acceleration mechanism have been identified at high latitudes by Wescott et al. (1976) and Mozer et al. (1977).

Since there is a westward electric field in the evening sector auroral oval (Mozer and Lucht, 1974) the electrons will follow $\underline{E} \times \underline{B}$ drift motion which will cause their equatorial plane crossings to move progressively earthward. Thus particles in the bps will gradually enter the cps and approach the inner edge of the plasma sheet. It then appears likely that, by the time the electrons have passed the boundary between the bps and the cps, many have been accelerated up to the keV energy range providing a spectrum ranging from eV to keV. Any subsequent energization would be caused by Fermi and betatron acceleration processes, and would be relatively minor. We therefore see the noise observed poleward of the eastward electrojet and in the poleward portion of the eastward electrojet as being associated with electron energization and the coincident production of discrete auroral arcs.

The diffuse aurora in the equatorward portion of the westward electrojet and any discrete arcs in this region do not necessarily have associated noise. Occasionally noise will be observed in this region but it is generally very low frequency with an upper frequency cutoff of ∿ 200 kHz. We therefore claim that *noise with frequencies up to ∿ 500 kHz (the local plasma frequency) is generated in the bps and is associated with discrete auroral arcs and 'inverted-V' structures in the energetic electron spectrograms.* Based on our study of the energetic electrons in Case 1, we would further claim that *the electron precipitation would have to feature monoenergetic fluxes of such intensity that there would be a positive slope in velocity space for electrons with energies above 1 keV.* We shall discuss the mechanisms for the production of the noise and the explanation of the phenomenology of the noise behaviour in the next section.

(ii) Mechanism for the Production of Noise in the Frequency Range

100 < f < 500 kHz

In searching for the source of noise in the kHz range, it is natural to seek some form of wave-particle interaction which can lead to the production of the noise in a manner which reflects the observed power levels. Some work on noise in the frequency range studied in this report has been carried out in the past. We note, in particular, the work of James (1973) who has shown that the experimentally observed power fluxes of VLF hiss in the dayside-cusp ionosphere are too large to be produced by incoherent Cerenkov radiation from precipitating electrons. Taylor and Shawhan (1974) have made a comparison of a very intense VLF hiss and an observed electron spectrum observed by Injun 5 spacecraft and found that the power expected from Cerenkov radiation are two orders of magnitude too small. They concluded that a partially

coherent or amplified Cerenkov source or an instability is possibly located in the altitude range 3,000 - 10,000 km. Maggs (1976) has calculated theoretical power flux levels of incoherent Cerenkov radiation limited by collisionless damping to be below 10^{-20} W/m^{2}Hz compared with observed fluxes as high as 10^{-11} W/m^{2}Hz (Gurnett and Frank, 1972).

In order to produce higher power fluxes, Swift and Kan (1975) have suggested that VLF hiss is produced by beam amplification of electrostatic whistlers. Maggs (1976) showed that indeed both the bandwidth and power fluxes of observed VLF hiss could be accounted for by convective beam amplification. In order to show this, he had to solve the wave kinetic equation for a model inhomogeneous ionosphere. Figure 28 shows a model arc Maggs used in his calculations. By modelling the arc as a narrow field-aligned beam of warm electrons with a drifting Maxwellian velocity distribution, the necessary range of positive slope in the velocity distribution could be produced in order to create the necessary convective growth of the incoherent Cerenkov radiation. The curvature of the source region in the east-west direction was simulted by a horizontal cutoff distance which, of course, would be a function of how active the arc is (see Figure 28). The electron beam was assumed to exist for several thousand kilometers along field lines.

His approach, however, was not valid for high frequencies (for the electron plasma frequency less than the electron gyrofrequency) due to non-linear processes. Maggs (1977) circumvented this problem by refracting the electrostatic waves out of the region of the auroral electron beam, thus limiting their amplification. As a result of this modification, Maggs was able to develop a graphical algorithm for predicting the power flux spectra of both whistler and upper hybrid noise for various beam and ionospheric
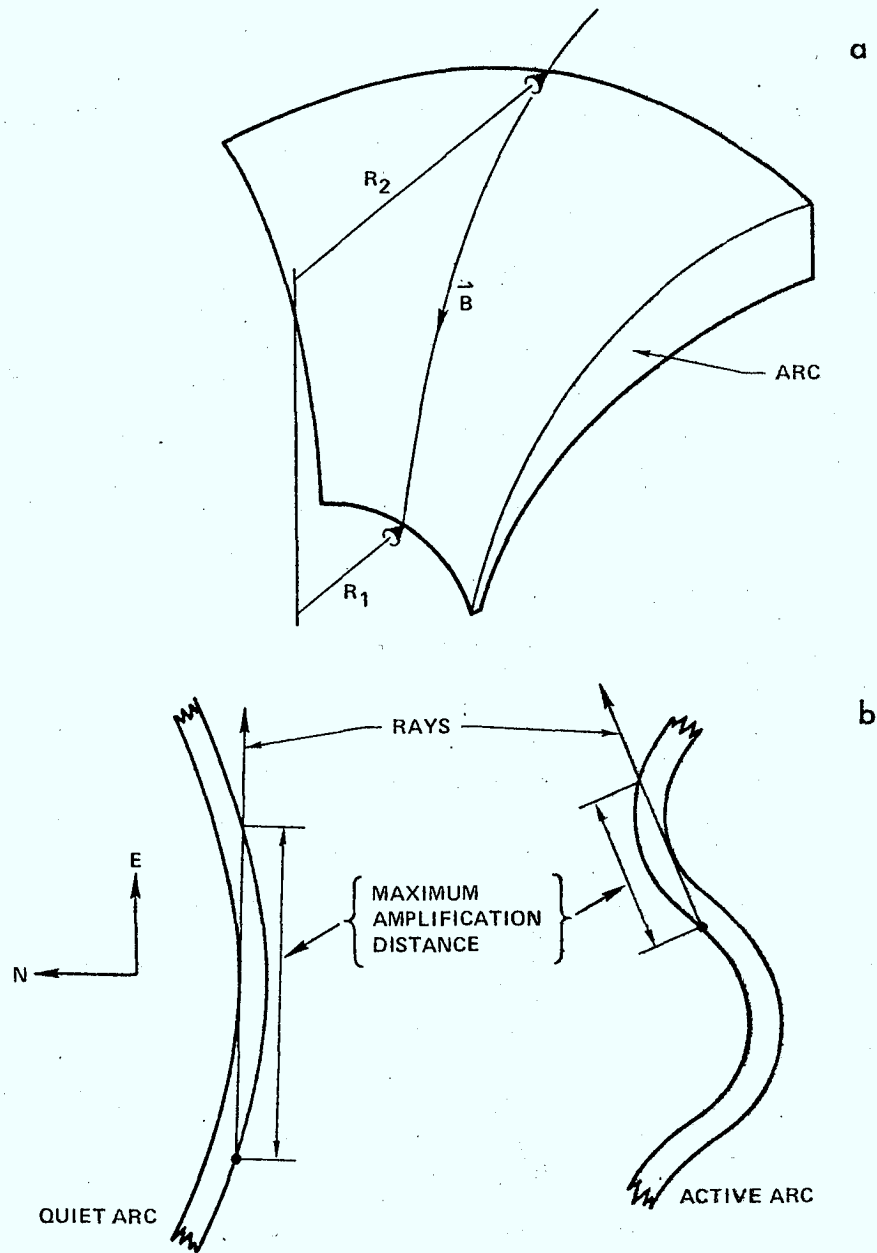
Figure 28: Model auroral arcs used by Maggs (1976); note the variation in horizontal scale between quiet arcs and active arcs and the influence of this on the maximum amplification distance.

parameters. This graphical algorithm is presently being applied to the noise spectra for Day 346, 1971. [Also, other events studied in this report will be processed in a similar fashion at a later date.]

Meng (1976) has catagorized three types of electron precipitation features for three auroral forms in the evening sector: a faint diffuse aurora, a faint discrete arc and a bright quiet arc. The faint discrete arc and bright quiet arc were found to have energetic electron spectral peaks at 0.5 - 1.2 keV and $\sim$ 3.2 keV respectively. Maggs (1976) believes that these monoenergetic beams produce the necessary positive slope in velocity space for the convective amplification process to take place. From the differential energy spectra of electrons shown in Case 1 (Figure 7) we have good reason to believe that the combination of adequate fluxes of energetic electrons coupled with a positive slope in velocity space are the conditions for the production of the noise observed using the AGC aboard ISIS 2. We would suggest that, for arcs in the equatorward portion of the eastward electrojet where no noise enhancements are observed, no positive slope in velocity space exists for the differential energy spectra. Thus, even though fluxes of energetic electrons may be high, the absence of the drifting Maxwellian ensures that no noise in the frequency range $100 < f < 500$ kHz would be produced.

The problem of determining the location and characteristics of the source region are compounded by the fact that the ray paths of electrostatic noises in an inhomogeneous ionosphere is extremely complicated. Therefore, the interpretation of the noise spectra as the satellite passes through the polar ionosphere, in terms of possible source regimes, is difficult, if not impossible (see James, 1973). In order to demonstrate this, two model source regions are presented in Figures 29 and 30. (J. E. Maggs, personal communication)
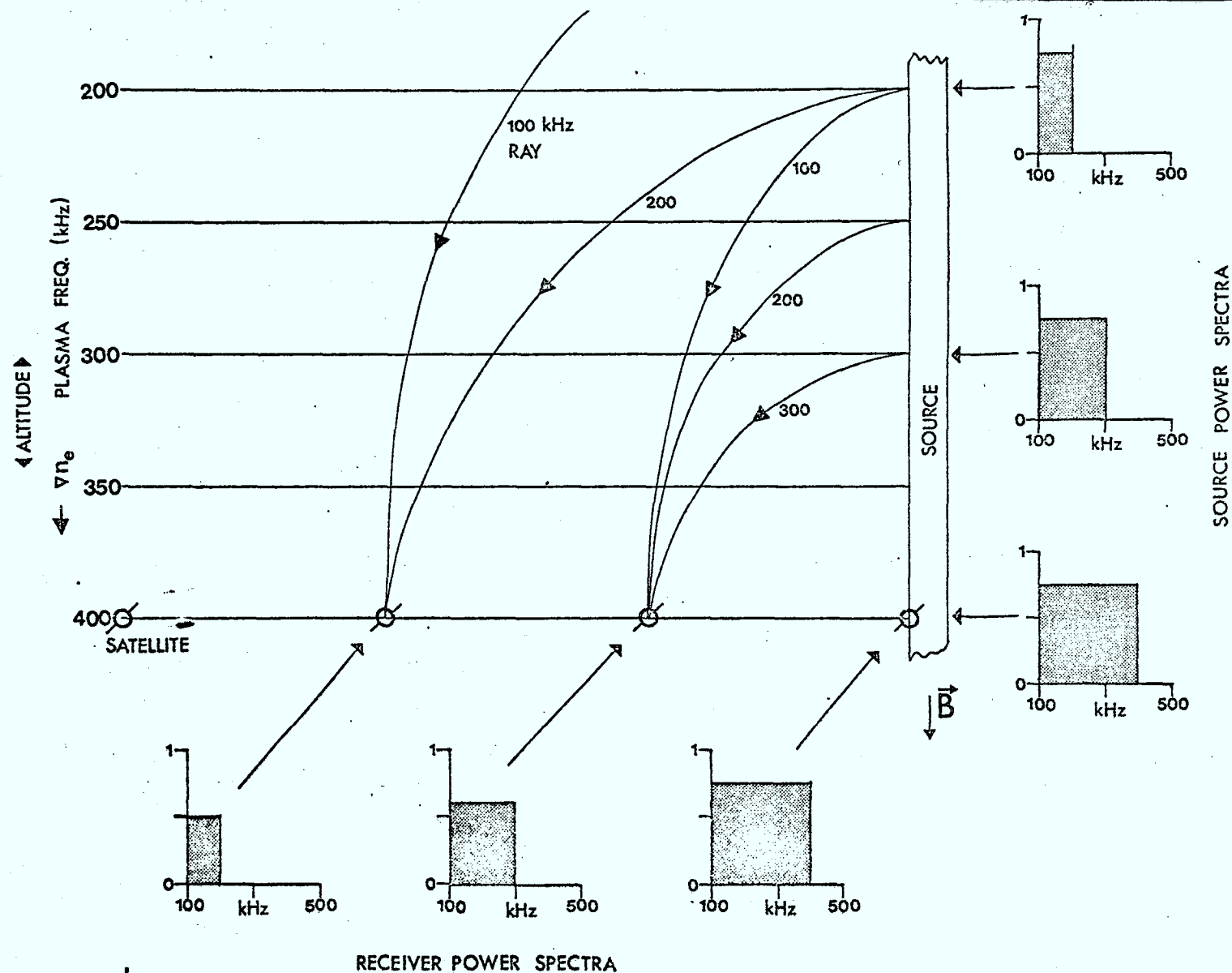
Figure 29: Schematic diagram showing the receiver power spectra as a function of distance from a hypothetical field-aligned source. The maximum frequency of the source is assumed to be the local plasma frequency, which is a function of altitude (i.e. ∇n_e in the direction of the magnetic field).
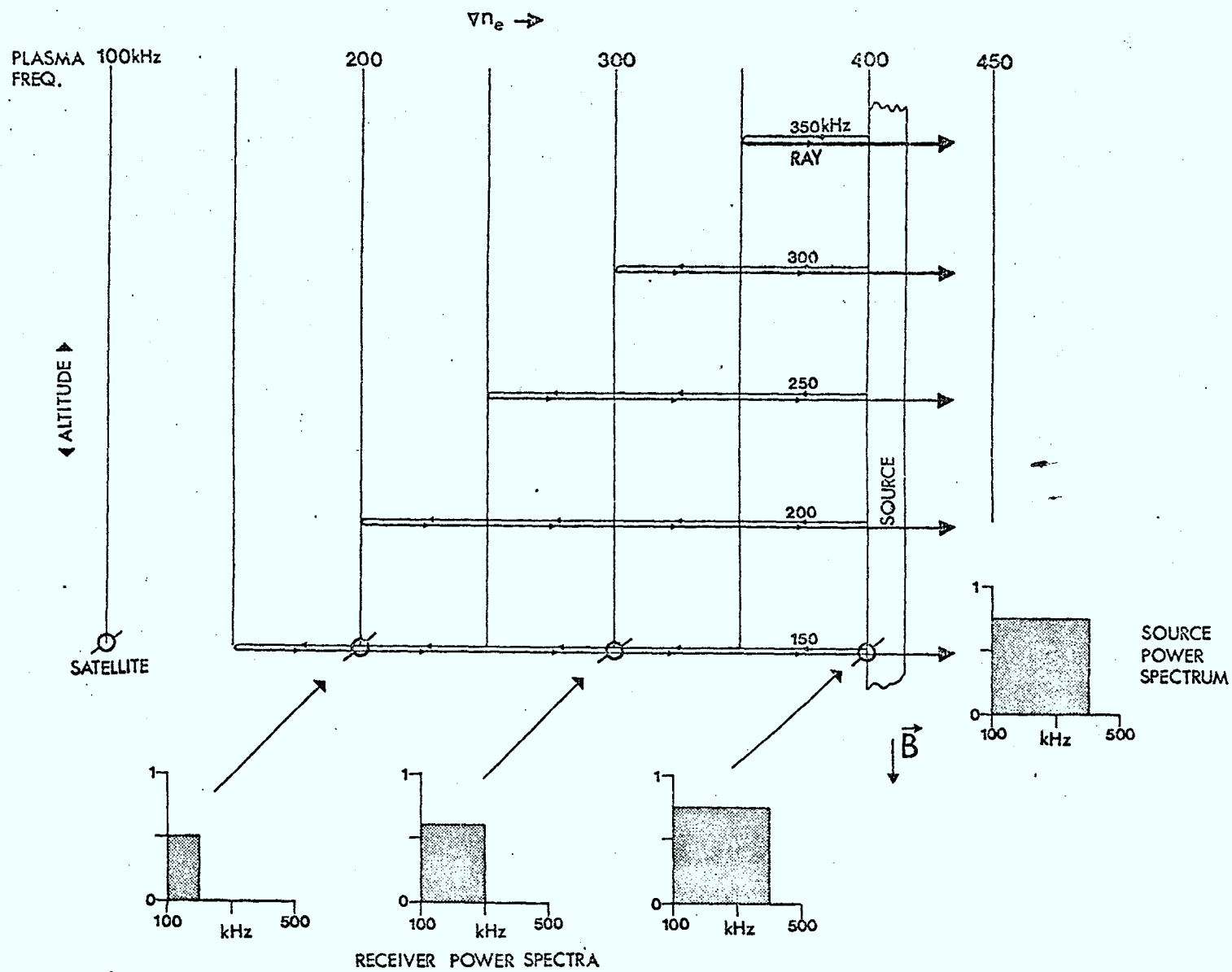
Figure 30: Same as Figure 29 except that ∇n_e is perpendicular to the magnetic field and the source power spectrum does not vary with altitude.

1977). In both cases the source is assumed to be aligned with the magnetic field direction. In Figure 29 the upper cutoff frequency of the source is made to vary with height as does the plasma frequency for the model ionosphere (i.e. ∇n_e is in the direction of the magnetic field).

As the satellite passes through the ionosphere the receiver power spectra would show an increase in amplitude as well as frequency. The reverse of this would be true as the satellite recedes from the source. This response is similar to that seen in most of the ISIS 2 passes. James (1973) also observed this same increase in the cutoff frequency of the receiver power spectra in the dayside-cusp ionosphere. However, Figure 30 illustrates a similar receiver response if ∇n_e is perpendicular to the magnetic field (horizontal gradients in the local plasma frequency). Such gradients would be generated by thermal plasma enhancements observed above the electrojet region by Rostoker et al. (1975a, 1976). [The ray paths for different frequencies were positioned at various heights only for convenience and does not represent a variation with altitude.] The receiver power spectra observed as the satellite moves away from the source would, of course, depend upon ∇n_e on the other side of the source. Since the polar ionosphere is known to have both horizontal and vertical components of ∇n_e, the problem of inferring the source can only be attempting by complicated ray tracing techniques (see James, 1973 and Maggs, 1976).

In summary, our data favor the model of Maggs (1976, 1977) which proposes that noise in the frequency range between the lower hybrid frequency and the local plasma frequency (or electron gyrofrequency, whichever is the lower) is produced by convective amplification of the whistler noise associated with beams of energetic electrons which feature a drifting Maxwellian.

Based on the data available for this study, we are unable to say for certain whether or not ISIS 2 is passing through the source region for the noise, although it is certain that the noise source is not below the satellite.

(iii) The Relationship of Noise to Thermal Plasma Enhancements in the
     Topside Ionosphere

In an earlier study for DOC, Rostoker et al. (1975a) showed that thermal plasma enhancements were observed in the evening sector centered roughly at the latitude of the poleward boundary of the eastward electrojet. The enhancements are due to O^+ being drawn up the field lines, possibly through the action of forces which result in the generation of the polarwind. Since this cold plasma is found in the same region as noise and field-aligned current in general terms, a more careful correlation was undertaken using the data shown in the bar chart presented in Figure 3. For the cases that are treated, it is clear that there are a significant number of cases where the thermal plasma lies outside the region of noise (e.g. Days 19 and 25, 1972) and also there are cases where noise lies outside the region of thermal plasma enhancement (e.g. Days 4 and 13, 1972). Thus, at any instant of time, there is clearly not a one-to-one correlation between noise in the kHz range and thermal plasma enhancements.

The lack of correlation can be understood in the following framework. The thermal plasma at high altitude stems from the precipitation of significant fluxes of low energy (a few hundred eV) which causes secondary ionization in the F-region of the ionosphere. The secondary electrons together with their associated ions (O^+) are drawn up the field lines to ISIS altitudes with some delay time. However, the noise is associated with the precipitating electrons,

and so there is a time lag between any noise burst and the arrival time at ISIS altitude of electrons created originally in the F-region by the primaries with which the noise burst is associated. Thus there is no reason to expect a correlation between noise and thermal plasma enhancements in the topside ionosphere due to the existence of the time lags discussed above.

(iv) The Relationship of Noise to Field-Aligned and Electrojet Current
   Flow in the Evening Sector

In discussing the phenomenon of field-aligned current flow, it is worth keeping in mind that no-one has ever measured ionospheric or magnetospheric currents directly; currents have always been inferred from magnetic measurements on the ground or aboard satellites, or from particle drift measurements in the context of some model atmosphere. Using these techniques Rostoker et al. (1975b), Kamide and Akasofu (1976) and Kamide and Rostoker (1977) have reached the conclusion that upward current flows in the poleward portion of the eastward electrojet and in the region immediately poleward of the eastward electrojet. Downward current flows in the equatorward portion of the eastward electrojet. In terms of magnetotail phenomenology, downward current flows from the cps and upward current flows into the bps.

Several workers have recently suggested that the upward current is carried in discrete arcs by downward moving energetic electrons (e.g. Kamide and Rostoker, 1977), although the electrons with energies above 0.5 keV may only be responsible for about 20% of this current (Casserley and Cloutier, 1975). Since most discrete arcs are found in the poleward portion of the eastward electrojet and north of its border where a westward electrojet is often observed, it is reasonable to contend that discrete arcs mark the regions of upward current flow.

We therefore contend that discrete arcs within the poleward portion and/or at the poleward border of the eastward electrojet are the site of the upward current flow which balances the downward current flow in the equatorward portion of that electrojet. Discrete arcs poleward of the eastward electrojet carry field-aligned current which stems from the diversion of the westward ionospheric current up the field lines. In effect this latter upward current constitutes part of the net field-aligned current flow in the evening sector. The balance of the net field-aligned current flow will stem from the eastward electrojet current which must diverge up the field lines as it flows towards the midnight sector. This upward current flow will probably occur at the boundary between the eastward electrojet and westward electrojet to the north, as there are marked gradients in both conductivity and electric field at that boundary (see Figure 2).

Insofar as the relationship between noise and net field-aligned current flow is concerned, Rostoker et al. (1975a) have used ground-based data to define the latitudinal regime of regions of net field-aligned current flow measured at the time of several of the ISIS 2 passes dealt with in our study. In Table 3 we show the latitude range spanned by the noise (amplitude greater than -70 db) and net field-aligned current for these events. For all cases except the westward electrojet near dawn, the noise is almost exactly contained within the region of net field-aligned current flow. Keeping in mind the error in estimation of noise onset (based on the time between sweeps) and the error in estimation of the latitudes at which the D-component (used to predict field-aligned current) begins its level change, we may say that noise in the frequency range $100 < f < 500$ kHz with amplitudes above ~ -70db is a good indicator of the present of net upward field-aligned current flow in the evening sector.

Table 3

Latitude Range Occupied by Noise
and by Net Field-Aligned Current Flow
for the ISIS Passes Treated in this Study

Year	Day	Time	Latitude Range of Field-Aligned Current	Latitude Range of Noise
1971	346	0609	67.5 - 72.5	67 - 72
1972	004	0527	70 - 76	69.5 - 74
	005	0412	72.5 - 76	72 - 74
	010	0334	70 - 76	69.5 - 75
	011	0410	71 - 76	72 - 76
	013	0333	70 - 75	71 - 76
	017	0409	65 - 70	66 - 72.5
	019	0332	70 - 75	72 - 74
	025	0331	67.5 - 72.5	69 - 74
	039	0250	67.5 - 72.5	66 - 75
	041	0213	73 - 77	71.5 - 76.5
	058*	1236	67.5 - 75	73.5 - 74.5

*westward electrojet near local dawn

We shall now speculate on the role which noise plays in the regulation of field-aligned current flow in the auroral oval. First we emphasize again the fact that noise, energetic electrons and upward field-aligned current appear to be colocated. The energetic electron spectrum in this region is that of an 'inverted V' which suggests that there is a potential drop along the field lines (Gurnett, 1972). As we have pointed out in the previous section, the satellite passes either through the region of potential drop or just under it. Since Mozer et al. (1977) have shown the region of potential drop to be highly turbulent, it is tempting to associate the noise with a source region through which the satellite flies. The observation by Shelley et al. (1976) of energetic ions coming up field lines from regions below 5000 km suggests, in fact, that ISIS 2 may well fly directly through the source region and therefore that the observed noise associated with the auroral arcs is detected by the ISIS spacecraft inside the source region.

In order to understand the relevance of noise to field-aligned current flow, it is necessary to understand the physics of the processes through which current is driven and noise is generated. While we have commented earlier on the noise generation processes proposed by Maggs (1976, 1977) it is useful to comment on the role of currents in the auroral oval. At the present time, it is felt that the electric field which drives current in the ionosphere originates in the magnetotail, and is related directly to the drift of particles in that region of space. Enhanced convection would lead to enhanced current flow across the auroral oval and correspondingly enhanced field-aligned current. While downward current flow in the equatorward portion of the oval can be carried by low energy electrons flowing out of the ionosphere, it would appear that the more intense currents in the poleward portion of the oval require

more energetic particles and hence some acceleration mechanism. We feel that
present evidence suggests that a double layer (Block, 1972) or oblique electro-
static shocks (Swift, 1975) is set up in the topside ionosphere which accel-
erates electrons downwards and ions upwards as the most likely acceleration
mechanisms. Basically, monoenergetic streams of electrons are simply a
consequence of the acceleration process which, in turn, regulates the field-
aligned current. As we have seen, however, it is the monoenergetic stream of
electrons (or rather a drifting Maxwellian distribution with a positive slope
in velocity space) which leads to the generation of noise. Therefore, the
noise is not quantitatively related to the current flow in any simple way;
it is simply a by-product of the processes through which upward field-aligned
current is driven.

It is also worth repeating that the higher noise frequencies are assoc-
iated with electrons with energies above ~ 1 keV. However, Casserly and
Cloutier (1975) suggest that only $\sim 20\%$ of the current is carried by electrons
with energies greater than ~ 0.5 keV, so that noise in the frequency range
$200 < f < 500$ kHz should not relate to the major portion of the upward field-
aligned current. Since, as we have pointed out earlier, the lower frequency
noise appears to relate to electrons with energies less than 1 keV, it may well
be that there is a quantitative relationship between noise near 100 kHz and
upward field-aligned current flow in the evening sector. However, any such
relationship cannot easily be established using solely ground based magneto-
meter data. It will be necessary to have _in situ_ measurements of magnetic
field from which to infer field-aligned current flow in order that a more
quantitative relationship between field-aligned currents and noise in the
kHz range can be established. It is hoped that the low altitude mission (LAM)

presently being proposed by the Canadian space science community will, among its accomplishments, provide the necessary data to quantitatively relate noise in the kHz frequency range to field-aligned current flow in the topside ionosphere.

Acknowledgements

References

Ackerson, K. L., and L. A. Frank, Correlated satellite measurements of low-energy electron precipitation and ground-based observations of a visible auroral arc, J. Geophys. Res., 76, 1128, 1972.

Alfvén, H., and C.-G. Fälthammar, Cosmic Electrodynamics, Oxford University Press, Oxford, 1963.

Block, L. P., Potential double layers in the ionosphere, Cosm. Electrodyn., 3, 349, 1972.

Block, L. P., Double Layers in Physics of the Hot Plasma in the Magnetosphere, ed. B. Hultqvist and L. Stenflow, pp 229, Plenum Press, New York, 1975.

Burch, J. L., W. Lennartsson, W. B. Hanson, R. A. Heelis, J. H. Hoffman and R. A. Hoffman. Properties of spikelike shear flow reversals observed in the auroral plasma by Atmospheric Explorer C, J. Geophys. Res., 81, 3886, 1976.

Burrows, J. R., The Plasma sheet in the evening sector, in Magnetospheric Physics, ed. by B. M. McCormac, p. 179, D. Reidel Publ. Co., Dordrecht-Holland, 1974.

Casserley, R. T., Jr., and P. A. Cloutier, Rocket-based magnetic observations of auroral Birkeland currents in association with a structural auroral arc, J. Geophys. Res., 80, 2165, 1975.

Evans, D. S., Precipitating electron fluxes formed by a magnetic field aligned potential difference, J. Geophys. Res., 79, 2853, 1974.

Frank, L. A. and K. L. Ackerson, Local time survey of plasma at low altitudes over the auroral zone, J. Geophys. Res., 76, 4116, 1972.

Gurnett, D. A., and L. A. Frank, VLF hiss and related plasma observations in the polar magnetosphere, J. Geophys. Res., 77, 172-190, 1972.

Gurnett, D. A., Electric fields and plasma observations in the magnetosphere in _Critical Problems of Magnetospheric Physics_, ed. by E. R. Dyer, Jr., p. 123, National Academy of Sciences, Washington, D.C., 1972.

Haerendel, G., and G. Paschmann, Entry of solar wind plasma into the magnetosphere, in _Physics of the Hot Plasma in the Magnetosphere_, ed. by B. Hultqvist and L. Stenflo, p. 23, Plenum Press, New York, 1975.

Hartz, T. R., Particle precipitation patterns, in _The Radiating Atmosphere_, ed. by B. M. McCormac, p. 225, Springer-Verlag, New York, 1971.

Hasegawa, A., Instabilities and non-linear processes in geophysics and astrophysics, Rev. Geophys. Space Phys., _12_, 273, 1974.

Heikkila, W. J., Penetration of particles into the polar cap and auroral regions in _Critical Problems of Magnetospheric Physics_, ed. by E. R. Dyer, Jr., p. 67, IUCSTP, c/o National Academy of Sciences, Washington D.C., 1972.

Heikkila, W. J. and R. J. Pellinen, Localized induced electric field within the magnetotail, J. Geophys. Res., _82_, 1610, 1977.

James, H. G., Whistler mode hiss at low and medium frequencies in the day side cusp ionosphere, J. Geophys. Res., _78_, 4578-4599, 1973.

Kamide, Y. and S.-I. Akasofu, The location of field-aligned currents with respect to discrete auroral arcs, J. Geophys. Res., _81_, 3999, 1976.

Kamide, Y., and G. Rostoker, The spatial relationship of field-aligned currents and auroral electrojets to the distribution of nightside auroras, J. Geophys. Res., in press, 1977.

Kisabeth, J. L., The dynamical development of the polar electrojets, Ph.D. Thesis, University of Alberta, Edmonton, Alberta Canada, 1972.

Lennartsson, W., On the magnetic mirroring as the basic cause of parallel electric fields, J. Geophys. Res., _81_, 5583, 1976.

Maggs, J. E., Coherent generation of VLF hiss, J. Geophys. Res., 81, 1707, 1976.

Maggs, J. E., Electrostatic noise generated by the auroral electron beam, J. Geophys. Res., submitted for publication, 1977.

Meng, C.-I., Simultaneous observations of low-energy electron precipitation and optical auroral arcs in the evening sector by the DMSP 32 satellite, J. Geophys. Res., 81, 2771, 1976.

Mozer, F.S., Observations of large parallel electric fields in the auroral ionosphere, Ann. Géophys., 32, 97, 1976.

Mozer, F. S., and P. Lucht, The average auroral zone electric field, J. Geophys. Res., 79, 1001, 1974.

Mozer, F. S., C. W. Carlson, M. K. Hudson, R. B. Torbert, B. Parady, J. Yatteau and M. C. Kelley, Observations of paired electrostatic shocks in the polar magnetosphere, Phys. Rev. Lett., In press, 1977.

Papadopoulos, K., A review of anomalous resistivity for the ionosphere, Rev. Geophys. Space Phys., 15, 113, 1977.

Paschmann, G., G. Haerendel, N. Sckopke, H. Rosenbauer and P. C. Hedgecock, Plasma and magnetic field characteristics of the distant polar cusp near local noon: the entry layer, J. Geophys. Res., 81, 2883, 1976.

Pilipp, W., and G. Morfill, The plasma mantle as the origin of the plasma sheet, in Magnetospheric Particle and Fields, ed. by B. M. McCormac, p. 55, D. Reidel Publ. Co., Dordrecht, The Netherlands, 1976.

Rosenbauer, H., H. Grünwaldt, M. D. Montgomery, G. Paschmann and N. Sckopke, Heos 2 plasma observations in the distant polar magnetosphere: the plasma mantle, J. Geophys. Res., 80, 2723, 1975.

Rostoker, G., J. C. Armstrong and A. J. Zmuda, Field-aligned current flow associated with the instrusion of the substorm intensified westward electrojet into the evening sector, J. Geophys. Res., 80, 3571, 1975b.

Rostoker, G., M. P. Hron and R. P. Sharma, Research on the correlation of Alouette-ISIS satellite data with ground based magnetometer data, Final Rept. Contract OSP3-0167, 83 pp, April, 1975a.

Rostoker, G., R. P. Sharma and M. P. Hron, Thermal plasma enhancements in the topside ionosphere and their relationship to the auroral electro-jets, Planet. Space Sci., 24, 1081, 1976.

Rostoker, G., K. Kawasaki, J. D. Winningham, J. R. Burrows and J. L. Kisabeth, Field-aligned current flow near the dusk meridian associated with the eastward auroral electrojet, Abstract, IAGA Assembly, Seattle, August, 1977.

Shelley, E. G., R. D. Sharp and R. G. Johnson, Satellite observations of an ionospheric acceleration mechanism, Geophys. Res. Lett., 3, 654, 1976.

Swift, D. W., On the formation of auroral arcs and the acceleration of auroral electrons, J. Geophys. Res., 80, 2096, 1975.

Swift, D. W., and J. R. Kan, A theory of auroral hiss and implications on the origin of auroral electrons, J. Geophys. Res., 80, 985-992, 1975.

Taylor, W. W. L., and S. D. Shawhan, A test of incoherent Cerenkov radiation for VLF hiss and other magnetospheric emissions, J. Geophys. Res., 79, 105-117, 1974.

Wallis, D. D., C. D. Anger, and G. Rostoker, The spatial relationship of the auroral electrojets and the visible aurora in the evening sector, J. Geophys. Res., 81, 2857, 1976.

Wescott, E. M., H. C. Stenbaek-Nielsen, T. Hallinen, T. N. Davis and H. M. Peek, The Skylab barium plasma injection experiments, 2. Evidence for a double layer, J. Geophys. Res., 81, 4495, 1976.

Wiens, R. G. and G. Rostoker, Characteristics of the development of the westward electrojet during the expansive phase of magnetospheric substorms, J. Geophys. Res., 80, 2109-2128, 1975.

Winningham, J. D., F. Yasuhara, S.-I. Akasofu and W. J. Heikkila, The latitudinal morphology of 10-eV to 10-keV electron fluxes during magnetically quiet and disturbed times at the 2100-0300 MLT sector, J. Geophys. Res., 80, 3148, 1975.

RESEARCH INTO CORRELATION OF ISIS 2
TOPSIDER SOUNDER AND ENERGETIC PARTI-
CLE DATE WITH GROUND-BASED...
--Rostoker, Gordon.

Date Due

FORM 109